Arbitrary order structure preserving discontinuous Galerkin methods for hyperbolic balance laws

Yulong Xing

Department of Mathematics
The Ohio State University
xing.205@osu.edu
https://people.math.osu.edu/xing.205/

Joint with G. Li (Qingdao Univ.), K. Wu (Southern Univ. of Sci. & Tech.), X. Zhang (Purdue Univ.), C.-W. Shu (Brown Univ.), W. Zhang, Y. Xu, Y. Xia (Univ. of Sci. & Tech. of China)

Seminar series "Hyperbolic equations: Structure preserving methods and other topics"
January 29th, 2021

THE OHIO STATE UNIVERSITY

Outline

Hyperbolic balance laws

- Hyperbolic balance laws (hyperbolic systems of conservation laws with source terms arising from geometrical, reactive, biological or other considerations):

$$U_t + f(U)_x = s(U, x)$$

- Applications in different fields including chemistry, biology, fluid dynamics, astrophysics, and meteorology.

- Examples: pollutant transport, sediment transport, chemical reaction, chemosensitive movement, shallow water flows, gas dynamics with gravity, nearly hydrostatic flow in climate modeling, etc.

Hyperbolic balance laws

- Hyperbolic balance laws

$$U_t + f(U)_x = s(U, x)$$

  Steady state solution, i.e. solution of $f(U)_x = s(U, x)$.

- Standard numerical schemes usually fail to capture the steady state well and introduce spurious oscillations. The grid must be extremely refined to reduce the size of these oscillations.

- Well-balanced methods are developed to reduce the unnecessarily refined mesh. They are specially designed to preserve exactly these steady-state solutions up to machine error with relatively coarse meshes.

A typical example of balance laws

Shallow water equations (SWEs) with a non-flat bottom topography:

$$h_t + (hu)_x = 0$$
$$(hu)_t + \left(hu^2 + \frac{1}{2}gh^2\right)_x = -ghb_x$$

- h : water height; u : velocity;
  b : bottom topography; g : gravitational constant.
- Still water at rest steady state:

$$u = 0 \qquad \text{and} \qquad h + b = const.$$

  Moving water steady state:

$$hu = const \qquad \text{and} \qquad u^2/2 + g(h + b) = const.$$

- Extensive well-balanced methods have been developed in the past two decades.

Numerical challenge

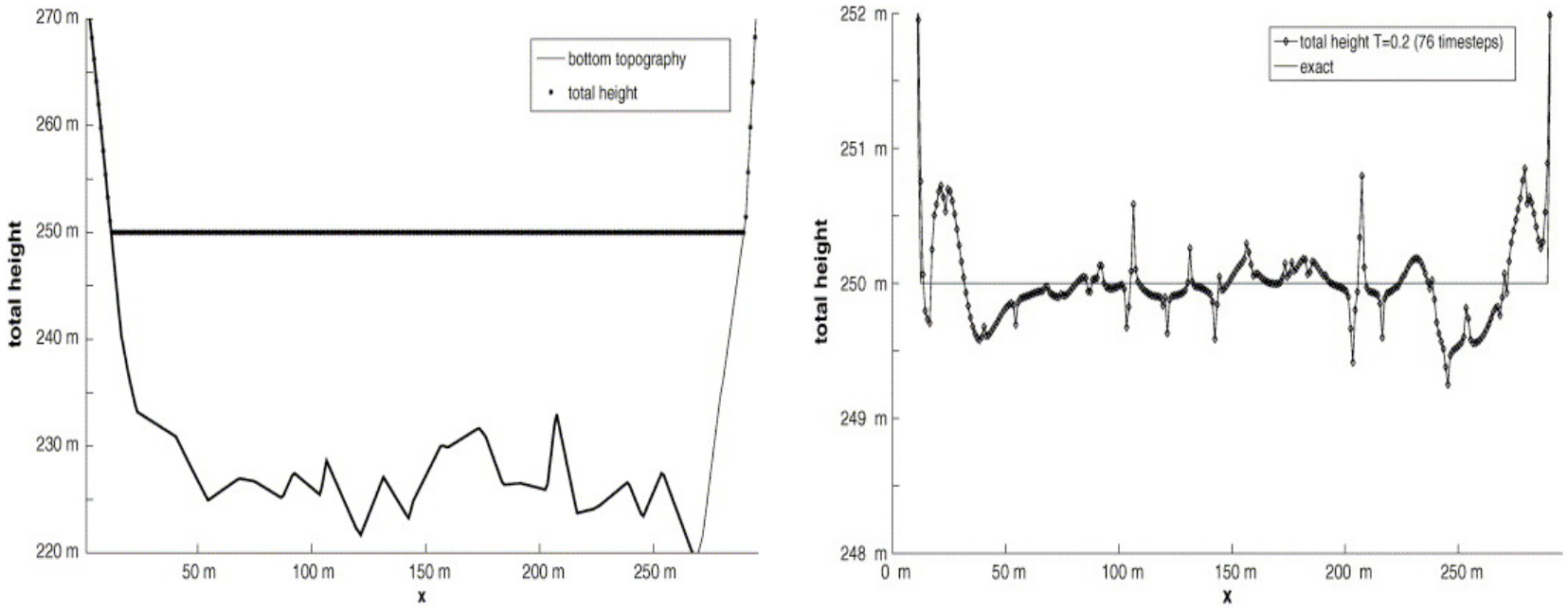

Figure: Numerical computation of Lake Rursee with 296 cells. Left: bottom topography and still water level at time $T = 0$; Right: water level at time $T = 0.2$ (76 time steps) by standard methods. Note the spurious oscillations on the right figure. (Credit: S. Noelle et al.)

Euler equations with a gravitational potential

Euler equations with a source term due to the static gravitational field:

$$\begin{aligned}
&\rho_t + \nabla \cdot (\rho \mathbf{u}) = 0, \\
&(\rho \mathbf{u})_t + \nabla \cdot (\rho \mathbf{u} \otimes \mathbf{u} + p \mathbf{I}_d) = -\rho \nabla \phi, \\
&E_t + \nabla \cdot ((E + p)\mathbf{u}) = -\rho \mathbf{u} \cdot \nabla \phi,
\end{aligned}$$

- ρ : fluid density; $\mathbf{u}$: velocity; p : pressure;
  $E = \frac{1}{2}\rho u^2 + p/(\gamma - 1)$: non-gravitational energy.

- $\phi = \phi(\mathbf{x})$: time independent gravitational potential.
  A simple example is: $\phi_z = g$.

- The hydrostatic balance with a zero velocity:

$$\rho = \rho(x), \qquad u = 0, \qquad \nabla p = -\rho \nabla \phi,$$

  where the flux produced by the pressure balances the gravitational source.

Small perturbation of the 2D equilibrium solution

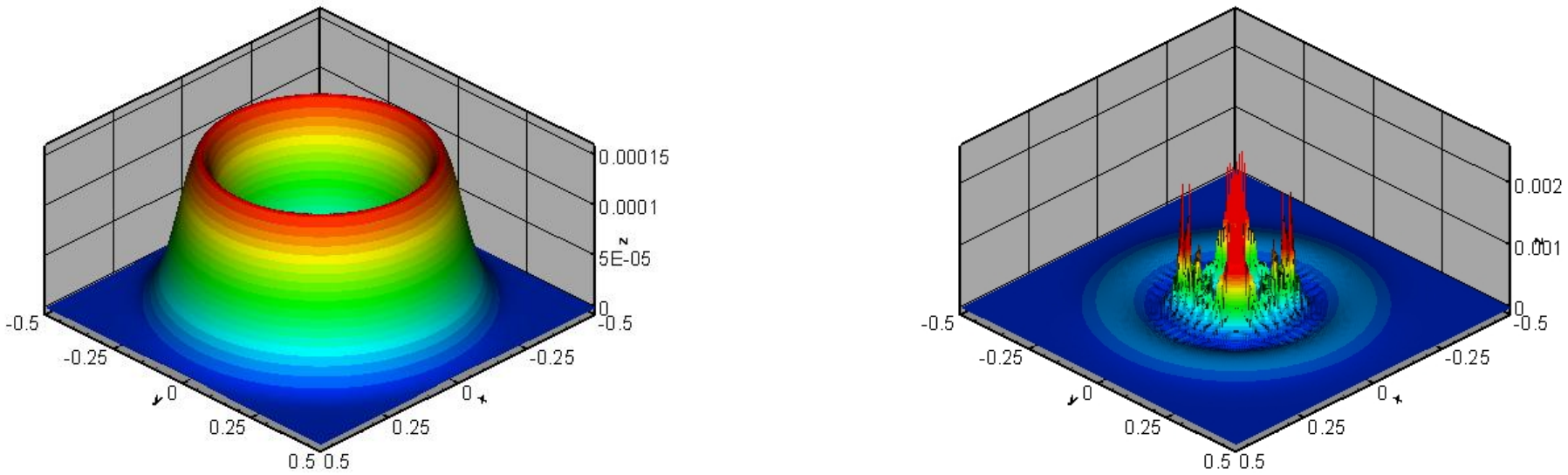

Figure: The 3D views of the velocity $\left(\sqrt{u^2+v^2}\right)$. Left: well-balanced methods; Right: non-well-balanced methods.

Structure preserving methods

Structure preserving methods

- Numerical partial differential equations (PDEs): Compute numerical approximation to the solutions of PDEs.

- Exact solutions of PDEs satisfy many continuum properties.
  Numerical solutions satisfy these properties "approximately", not exactly.

Structure preserving methods

- Numerical partial differential equations (PDEs): Compute numerical approximation to the solutions of PDEs.

- Exact solutions of PDEs satisfy many continuum properties.
  Numerical solutions satisfy these properties "approximately", not exactly.

- Structure/Feature Preserving methods:
  Preserve the structure or other fundamental continuum property of the underlying problems in the discrete level.

  Goal:
  (Hopefully) produce a more accurate numerical approximation than with general-purpose methods, on relatively coarse meshes.

Structure preserving methods for PDEs

Conserved quantities:

- Energy,
- Hamiltonian,
- Momentum - angular, linear,
- Symmetry,
- ...

Structure preserving methods for PDEs

Conserved quantities:

- Energy,
- Hamiltonian,
- Momentum - angular, linear,
- Symmetry,
- ...

Other continuum properties of PDEs:

- Positivity,
- Maximum principle,
- Divergence free $\nabla \cdot \mathbf{B} = 0$,
- Asymptotic behavior,
- ...

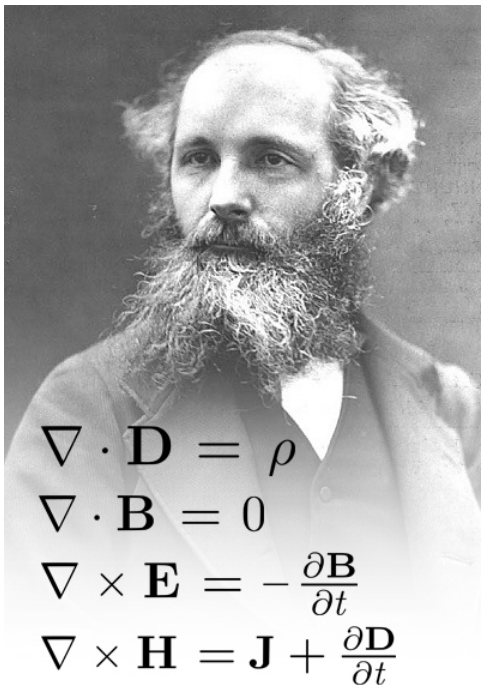

Examples of structure preserving methods for PDEs

- Mass conservation methods for conservation laws
- Energy conserving, Hamiltonian conserving methods
- Angular momentum, vorticity preserving methods
- Bound preserving, positivity preserving methods
- Symmetry preserving methods
- Globally divergence free methods
- Entropy stable, entropy consistent methods to satisfy the entropy condition
- Asymptotic preserving methods to preserve the asymptotic limit
- Well-balanced methods to preserve the equilibrium state
- ...

Discontinuous Galerkin methods

Discontinuous Galerkin (DG) methods

To solve

$$u_t + u_x = 0$$
$$\Downarrow$$
$$u_t v + u_x v = 0$$
$$\Downarrow$$
$$\int_I u_t v dx + \int_I u_x v dx = 0, \qquad \text{on } I = (x_L, x_R)$$
$$\Downarrow$$
$$\int_I u_t v dx - \int_I u v_x dx + uv(x_R) - uv(x_L) = 0, \qquad \text{on } I = (x_L, x_R)$$

Weak formulation!

DG methods

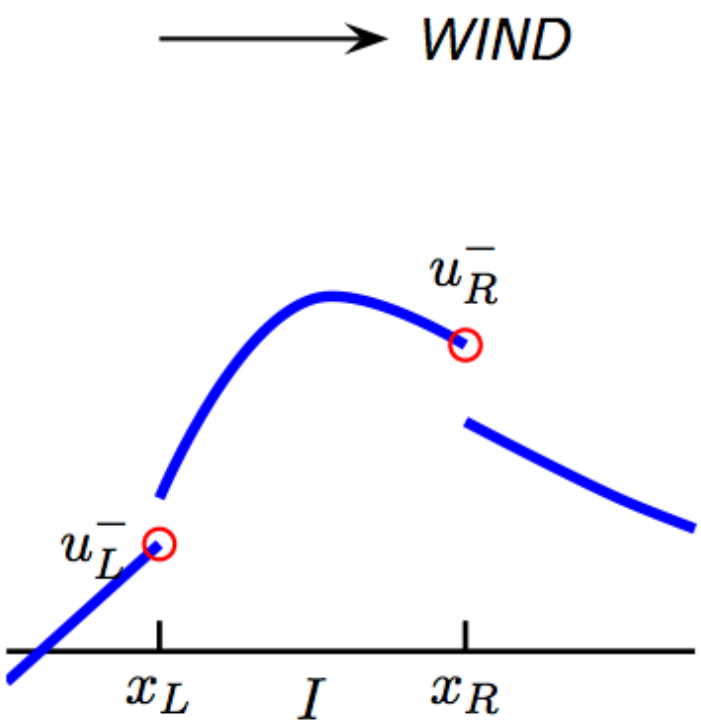

Find $u \in V_h$= piecewise polynomial space, s.t. for any $v \in V_h$,

$$\int_I u_t v \, dx - \int_I u v_x \, dx$$
$$+\hat{u}v^-(x_R) - \hat{u}v^+(x_L) = 0.$$

Numerical Fluxes

$$\hat{u} = u^-.$$

Literature of DG methods

- First introduced by Reed and Hill (1973) for neutron transport equation, Lesaint and Raviart (1974).
- For elliptic problems: Babuska et al. (1973), Baker (1977), Wheeler (1978), Arnold (1979), Arnold et al. (2002), Cockburn et al. (2008) $\cdots$
- For parabolic problems: Bassi and Rebay (1997), Cockburn and Shu (1998) $\ldots$
- Runge Kutta DG (RKDG) for hyperbolic conservation problems: Cockburn and Shu (1989-1998) $\cdots$

The main objective

Develop high order accurate well-balanced discontinuous Galerkin schemes for the shallow water equations and Euler equations with source terms, which have the key advantage

- High order accuracy;
- Well-balanced for the steady state solutions;
- Positivity-preserving for the important physical quantities (e.g., water height, density, internal energy);
- Good resolution for smooth and discontinuous solutions.

We expect well-balanced methods to be efficient for time dependent near-equilibrium problems, and to behave similar as standard DG methods when far away from equilibrium.

Recent paper: Veiga, Abgrall, Teyssier (2018), Capturing near-equilibrium solutions: a comparison between high-order discontinuous Galerkin methods and well-balanced schemes

Euler equations with a gravitational potential

Euler equations with a source term due to the static gravitational field:

$$\begin{aligned}
&\rho_t + \nabla \cdot (\rho \mathbf{u}) = 0, \\
&(\rho \mathbf{u})_t + \nabla \cdot (\rho \mathbf{u} \otimes \mathbf{u} + p \mathbf{I}_d) = -\rho \nabla \phi, \\
&E_t + \nabla \cdot ((E + p)\mathbf{u}) = -\rho \mathbf{u} \cdot \nabla \phi,
\end{aligned}$$

- ρ : fluid density; $\mathbf{u}$: velocity; p : pressure;
  $E = \frac{1}{2}\rho u^2 + p/(\gamma - 1)$: non-gravitational energy.

- $\phi = \phi(\mathbf{x})$: time independent gravitational potential.
  A simple example is: $\phi_z = g$.

- The hydrostatic balance with a zero velocity:

$$\rho = \rho(x), \qquad u = 0, \qquad \nabla p = -\rho \nabla \phi,$$

  where the flux produced by the pressure balances the gravitational source.

Motivation and existing approaches

- Motivation: core-collapse supernova simulation

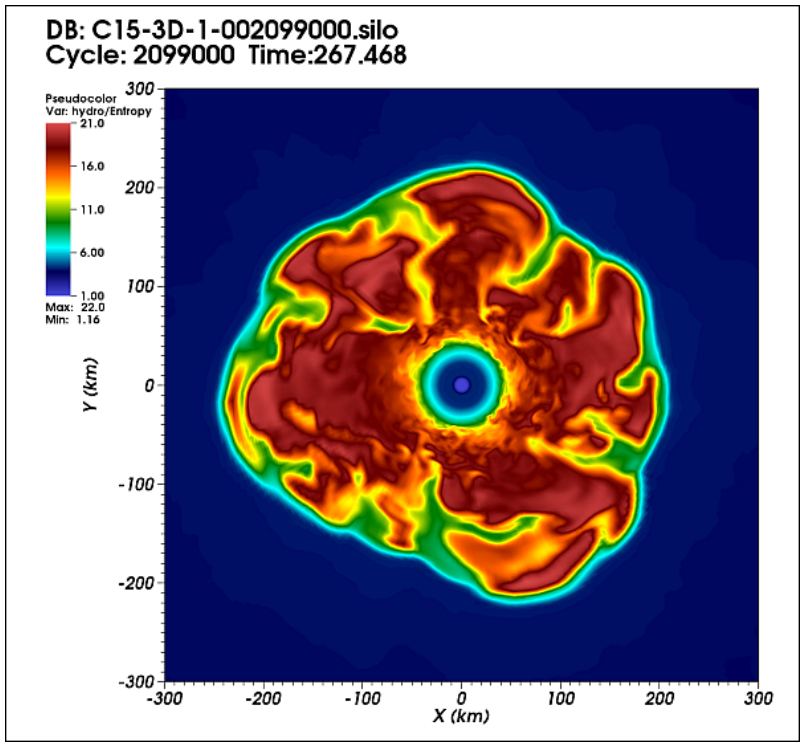

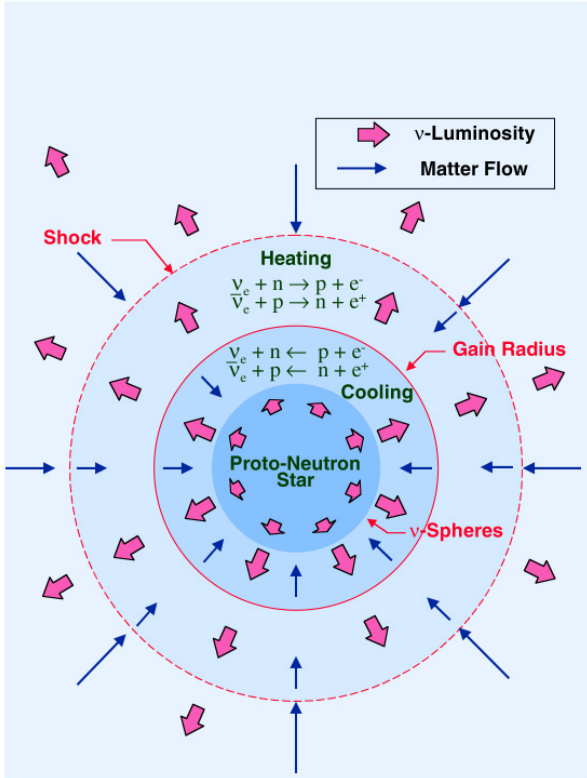

Figure: Image credit: Left: Endeve, Mezzacappa et al. (ORNL); Right: TeraScale Supernova Initiative.

- Many astrophysical problems involve the hydrodynamical evolution in a gravitational field. It is essential to correctly capture the effect of gravitational force in the simulations.

Motivation and existing approaches

- Other applications:
  1. Stellar "evolution": Stars evolve mostly quietly, very close to a hydrostatic state.
  2. Waves in stellar atmospheres: The wave amplitude may be much smaller when compared to the stratification from gravity...
  3. Atmospheric flows: Atmospheric motions happen on a hydrostatic background.

Motivation and existing approaches

- Other applications:
  1. Stellar "evolution": Stars evolve mostly quietly, very close to a hydrostatic state.
  2. Waves in stellar atmospheres: The wave amplitude may be much smaller when compared to the stratification from gravity...
  3. Atmospheric flows: Atmospheric motions happen on a hydrostatic background.
- Improper treatment of the gravitational force can introduce large spurious oscillations, unless the grid is extremely refined.

Motivation and existing approaches

- Some attempts in designing well-balanced methods for the Euler equations.

  LeVeque and Bale 1998
  Botta, Klein, Langenberg and Lützenkirchen 2004
  Xu and his collaborators 2007, 2010, 2011
  Xing, Shu, Li, 2013, 2015, 2016, 2018, 2020
  Käppeli and Mishra 2014, 2016, 2019
  Chandrashekar, Klingenberg, Puppo et. al. 2015, 2017-2020
  Chertock, Cui, Kurganovz, Özcan and Tadmor 2018
  Chen, Noelle 2019
  Veiga, Abgrall, Teyssier 2018
  ...

Steady state solutions

- The hydrostatic balance with a zero velocity:

$$\rho = \rho(x), \qquad u = 0, \qquad p_x = -\rho\phi_x,$$

where the flux produced by the pressure balances the gravitational source. Two important special steady state are the constant entropy (isentropic/polytropic) and constant temperature (isothermal) hydrostatic equilibrium states

- Isothermal equilibrium: For an ideal gas, we have $p = \rho RT$. The equilibrium (with constant temperature T_0) becomes

$$\rho = \rho_0 \exp\left(-\frac{\phi}{RT_0}\right), \quad u = 0, \quad p = RT_0\rho = p_0 \exp\left(-\frac{\phi}{RT_0}\right).$$

A special case with a linear gravitational potential field: $\phi_x = g$ is:

$$\rho = \rho_0 \exp(-g\rho_0 x/p_0), \qquad \mathbf{u} = 0, \qquad p = p_0 \exp(-g\rho_0 x/p_0).$$

Steady state solutions

- Polytropic equilibrium:

$$p = K\rho^{\gamma},$$

which will lead to the form of

$$\rho = \left(\frac{\gamma-1}{K\gamma}(C-\phi)\right)^{\frac{1}{\gamma-1}}, \qquad \mathbf{u} = 0, \qquad p = \frac{1}{K^{\frac{1}{\gamma-1}}}\left(\frac{\gamma-1}{\gamma}(C-\phi)\right)^{\frac{\gamma}{\gamma-1}},$$

or equivalently,

$$h + \phi = const,$$

where $h = e + p/\rho$ is the specific enthalpy and e is the specific internal energy.

A special case with a linear gravitational potential field: $\phi_x = g$ is:

$$p = p_0^{\frac{1}{\gamma-1}}\left(p_0 - \frac{\gamma-1}{\gamma}g\rho_0 x\right)^{\frac{\gamma}{\gamma-1}}, \qquad u = 0, \qquad \rho = \rho_0\left(\frac{p}{p_0}\right)^{\frac{1}{\gamma}}.$$

Key idea of well-balanced methods

- Discretize the source terms using an approximation consistent with that of approximating the flux derivative terms.
- This idea was adopted from Xing-Shu JSC 2006, that presented well-balanced methods for a family of balance laws satisfying

  (a): The steady state solution U that we are interested to preserve satisfies

  $$a(U, x) = constant$$

  for a known function $a(u, x)$.

  (b): The source term $s(U, x)$ can be decomposed as

  $$s(U, x) = \sum_i s_i(a(U, x))\, t_i'(x)$$

  for some functions s_i and t_i.

  Examples: Shallow water equations, Nozzle flow, Chemosensitive Movement, etc.

Equivalent form

- The simple steady state

$$\rho = c\exp(-gx), \qquad u = 0, \qquad p = c\exp(-gx),$$

with $\phi_x = g$ will be used as an example to illustrate the idea.

- Rewrite the equations as

$$\begin{aligned}
&\rho_t + (\rho u)_x = 0 \\
&(\rho u)_t + (\rho u^2 + p)_x = \frac{\rho}{\exp(-gx)}(\exp(-gx))_x \\
&E_t + ((E+p)u)_x = -\rho u g,
\end{aligned}$$

Purpose: introduce the derivative term in the source term, which can be treated in the similar way as the flux term.

- Denote them by

$$U_t + F(U)_x = S(U, \phi).$$

Semi-discrete DG scheme

$$U_t + F(U)_x = S(U, \phi).$$

- The semi-discrete DG scheme

$$\int_{I_j} (U_h)_t v \mathrm{d}x - \int_{I_j} F(U_h) v_x \mathrm{d}x + \hat{F}_{j+\frac{1}{2}} v(x^-_{j+\frac{1}{2}}) - \hat{F}_{j-\frac{1}{2}} v(x^+_{j-\frac{1}{2}}) = \int_{I_j} S v \mathrm{d}x,$$

  where

$$\widehat{F}_{j+\frac{1}{2}} = f(U_h(x^-_{j+\frac{1}{2}}, t), U_h(x^+_{j+\frac{1}{2}}, t)),$$

  and $f(a_1, a_2)$ is a numerical flux.

- Lax-Friedrichs flux, or any other numerical flux:

$$f(a_1, a_2) = \frac{1}{2}(F(a_1) + F(a_2) - \alpha(a_2 - a_1)).$$

Well-balanced source term approximation

- We first decompose the integral of the source term in the second equation as

$$\int_{I_j} S_2 v \mathrm{d}x = \int_{I_j} \rho \exp(gx) \left(\exp(-gx)\right)_x v \mathrm{d}x = \int_{I_j} \frac{\rho}{b} b_x v \mathrm{d}x$$

$$= \frac{\rho(x_j)}{b(x_j)} \left(b(x^-_{j+\frac{1}{2}}) v(x^-_{j+\frac{1}{2}}) - b(x^+_{j-\frac{1}{2}}) v(x^+_{j-\frac{1}{2}}) - \int_{I_j} b v_x \mathrm{d}x \right) + \int_{I_j} \left(\frac{\rho}{b} - \frac{\rho(x_j)}{b(x_j)} \right) b_x v \mathrm{d}x,$$

  where $b(x) = \exp(-gx)$.

- Let $b_h(x)$ be the projection of $b(x)$ into V_h^k, approximate the integral by:

$$\int_{I_j} S_2 v \mathrm{d}x \approx \int_{I_j} \left(\frac{\rho_h}{b_h} - \frac{\rho_h(x_j)}{b_h(x_j)} \right) (b_h)_x v \mathrm{d}x$$

$$+ \frac{\rho_h(x_j)}{b_h(x_j)} \left(\{b_h\}(x_{j+\frac{1}{2}}) v(x^-_{j+\frac{1}{2}}) - \{b_h\}(x_{j-\frac{1}{2}}) v(x^+_{j-\frac{1}{2}}) - \int_{I_j} b_h v_x \mathrm{d}x \right).$$

- Use quadrature rule to approximate the source term in the third equation

$$\int_{I_j} S_3 v \mathrm{d}x \approx \int_{I_j} -(\rho u)_h g v \mathrm{d}x.$$

Well-balanced fix to the numerical flux

- Lax-Friedrichs flux:

$$f(a_1, a_2) = \frac{1}{2}(F(a_1) + F(a_2) - \alpha(a_2 - a_1)).$$

$\alpha(a_2 - a_1)$ contributes to the numerical viscosity term, but may destroy the well-balanced property at the steady state.

- Well-balanced modification:

$$\hat{F}_{j+1/2} = \frac{1}{2}\left[F\left(U_h(x^-_{j+1/2})\right) + F\left(U_h(x^+_{j+1/2})\right) - \alpha'\left(\frac{U_h(x^+_{j+1/2})}{b_h(x^+_{j+1/2})} - \frac{U_h(x^-_{j+1/2})}{b_h(x^-_{j+1/2})}\right)\right].$$

To maintain enough artificial numerical viscosity:

$$\alpha' = \alpha \max_x b_h(x),$$

At the steady state, the numerical flux reduces to

$$\hat{f}_{j+\frac{1}{2}} = \frac{1}{2}\left[f\left(U(x^-_{j+1/2})\right) + f\left(U(x^+_{j+1/2})\right)\right].$$

Main result

Proposition: For the Euler equations with the linear gravitational potential field, the semi-discrete DG methods mentioned above can maintain the original high order accuracy and are well-balanced for the steady state solution.

Proof: At the steady state, we have

$$\rho_h = cb_h, \qquad u = 0, \qquad p_h = cb_h.$$

For the momentum equation, the source term approximation becomes

$$\int_{I_j} S_2 v \mathrm{d}x \approx c \left(\{b_h\}(x_{j+\frac{1}{2}}) v(x^-_{j+\frac{1}{2}}) - \{b_h\}(x_{j-\frac{1}{2}}) v(x^+_{j-\frac{1}{2}}) - \int_{I_j} b_h v_x \mathrm{d}x \right).$$

Since $u = 0$, the flux term $F_2 = \rho u^2 + p$ reduces to $p = cb$. Its numerical approximation takes the form of

$$\hat{F}_2(x_{j+\frac{1}{2}}) v(x^-_{j+\frac{1}{2}}) - \hat{F}_2(x_{j-\frac{1}{2}}) v(x^+_{j-\frac{1}{2}}) - \int_{I_j} F_2 v_x \mathrm{d}x$$

$$= c\{b_h\}(x_{j+\frac{1}{2}}) v(x^-_{j+\frac{1}{2}}) - c\{b_h\}(x_{j-\frac{1}{2}}) v(x^+_{j-\frac{1}{2}}) - \int_{I_j} cb_h v_x \mathrm{d}x.$$

General steady state

$$\rho = \rho^e(x), \qquad u = 0, \qquad p = p^e(x)$$

including (but not limited to) isothermal and polytropic equilibria

- We first rewrite the equations:

$$\rho_t + (\rho u)_x = 0,$$
$$(\rho u)_t + \left(\rho u^2 + p\right)_x = \frac{\rho}{\rho^e(x)} \left(p^e(x)\right)_x,$$
$$E_t + ((E+p)u)_x = -\rho u \phi_x,$$

- Well-balanced source term approximation:

$$\int_{I_j} S_2 v \mathrm{d}x \approx \int_{I_j} \left(\frac{\rho_h}{\rho^e} - \frac{\rho_h(x_j)}{\rho^e(x_j)}\right) (p^e)_x v \mathrm{d}x$$
$$+ \frac{\rho_h(x_j)}{\rho^e(x_j)} \left(\{p^e\}(x_{j+\frac{1}{2}}) v(x^-_{j+\frac{1}{2}}) - \{p^e\}(x_{j-\frac{1}{2}}) v(x^+_{j-\frac{1}{2}}) - \int_{I_j} p^e v_x \mathrm{d}x \right)$$

- Well-balanced fix to the numerical flux.

$$\hat{F}_{j+1/2} = \frac{1}{2}\left[F\left(U_h(x^-_{j+1/2})\right) + F\left(U_h(x^+_{j+1/2})\right) - \alpha' \left(\tilde{U}_h(x^+_{j+1/2}) - \tilde{U}_h(x^-_{j+1/2}) \right) \right]$$

with $\widetilde{U} = (\rho/\rho^e(x), \rho u/\rho^e(x), E/p^e(x))$.

Multi-dimensional Euler equations

- The Euler equations with a static gravitational field are

$$\begin{aligned}
&\rho_t + \nabla \cdot (\rho \mathbf{u}) = 0, \\
&(\rho \mathbf{u})_t + \nabla \cdot (\rho \mathbf{u} \otimes \mathbf{u} + p \mathbf{I}_d) = -\rho \nabla \phi, \\
&E_t + \nabla \cdot ((E + p)\mathbf{u}) = -\rho \mathbf{u} \cdot \nabla \phi,
\end{aligned}$$

- General hydrostatic balance:

$$\rho = \rho^e(x), \qquad \mathbf{u} = 0, \qquad p = p^e(x)$$

- Isothermal equilibrium

$$\rho = \rho_0 \exp\left(-\frac{\phi}{RT}\right), \qquad \mathbf{u} = 0, \qquad p = RT\rho = RT\rho_0 \exp\left(-\frac{\phi}{RT}\right),$$

  with constant temperature T.

Well-balanced methods

$$\rho = \rho^e(x), \qquad \mathbf{u} = 0, \qquad p = p^e(x)$$

including (but not limited to) isothermal and polytropic equilibria

- We first rewrite the source term:

$$-\rho\nabla\phi = \frac{\rho}{\rho^e(x)}\nabla p^e(x)$$

- Well-balanced source term approximation:

$$\int_K S_2 w \,\mathrm{d}x \approx \int_K \left(\frac{\rho_h}{\rho^e} - \frac{\rho_h(\mathbf{x}_K^0)}{\rho^e(\mathbf{x}_K^0)}\right)\nabla p^e \, w \,\mathrm{d}\mathbf{x} + \frac{\rho_h(\mathbf{x}_K^0)}{\rho^e(\mathbf{x}_K^0)}\left(\sum_{i=1}^m \int_{e_K^i} \{p^e(\mathbf{x})\}\nu_K^i w \,\mathrm{d}s - \int_K p^e \,\nabla w \,\mathrm{d}\mathbf{x}\right)$$

- Well-balanced fix to the numerical flux.

$$\hat{F}_{j+1/2} = \frac{1}{2}\left[F\left(U_h(x^-_{j+1/2})\right) + F\left(U_h(x^+_{j+1/2})\right) - \alpha'\left(\tilde{U}_h(x^+_{j+1/2}) - \tilde{U}_h(x^-_{j+1/2})\right)\right]$$

with $\widetilde{U} = (\rho/\rho^e(x), \rho u/\rho^e(x), E/p^e(x))$.

Well-balanced approach via hydrostatic reconstruction

Well-balanced methods for the polytropic balance

Key idea:

Decompose the solution into equilibrium and non-equilibrium parts, and treat them differently.

Well-balanced methods for the polytropic balance

Key idea:

Decompose the solution into equilibrium and non-equilibrium parts, and treat them differently.

Components:

- Recovery of well-balanced states;
- Decomposition of the solutions into equilibrium and non-equilibrium parts;
- Numerical fluxes via hydrostatic reconstruction;
- Novel source term approximation.

Use 1D Euler equation as example to demonstrate the algorithm.

Recovery of well-balanced states

Suppose $U(x, t = 0) = U^0(x)$ are in perfect equilibrium, i.e.,

$$u^0(x) = 0, \qquad h(x) + \phi(x) = const\, C.$$

- Initial condition for DG methods is the projection of these to $V_{\Delta x}$.
- Usually L^2 projection is used. But it is difficult to retrieve the constant C from the projected initial condition.
- This is straightforward in the finite difference framework.
- In our previous FV work for the shallow water equations, we define it as a solution of a nonlinear equation and solve it using Newton's iteration.

Recovery of well-balanced states

Suppose $U(x,t=0)=U^0(x)$ are in perfect equilibrium, i.e.,

$$u^0(x)=0, \qquad h(x)+\phi(x)=const\, C.$$

- DG methods are more flexible.
  We define Projection $P_h^+\omega$ as a projection of $\omega(x)$ into $V_{\Delta x}$:

$$\int_{I_j} P_h^+\omega v dx = \int_{I_j} \omega v dx,$$

  for any $v\in P^{k-1}$ on I_j, and

$$P_h^+\omega(x^+_{j-\frac{1}{2}})=\omega(x_{j-\frac{1}{2}}) \quad \text{at the left boundary } x_{j-\frac{1}{2}}.$$

- We can verify this projection is optimal, i.e., $\|P_h^+U(x)-U(x)\|=O(h^{k+1})$, plus we have

$$h(p_h(x_{j-\frac{1}{2}}),\rho_h(x_{j-\frac{1}{2}}))+\phi_h(x_{j-\frac{1}{2}})=const\, C,$$

  where $U_h(x)=P_h^+U(x)$, $\rho_h(x)=P_h^+\rho(x)$ etc.

Decomposition into equilibrium and non-equilibrium parts

- Key idea: decompose U_h into the sum of a reference equilibrium state U_h^e and the remaining part U_h^r.

Decomposition into equilibrium and non-equilibrium parts

- Key idea: decompose U_h into the sum of a reference equilibrium state U_h^e and the remaining part U_h^r.
- $U_h^e(x)$? (Recover the (projected) equilibrium at the steady state)

Decomposition into equilibrium and non-equilibrium parts

- Key idea: decompose U_h into the sum of a reference equilibrium state U_h^e and the remaining part U_h^r.
- $U_h^e(x)$? (Recover the (projected) equilibrium at the steady state)

  Let $h^e(x) = h(p_h(x_{j-\frac{1}{2}}), \rho_h(x_{j-\frac{1}{2}})) + \phi_h(x_{j-\frac{1}{2}}) - \phi(x)$. Recover $\rho^e(x)$ and $p^e(x)$ from $h^e(x)$. For the ideal gas law, we have the polytropic form

$$\rho^e(x) = \left(\frac{1}{K}\frac{\gamma-1}{\gamma}h^e(x)\right)^{\frac{1}{\gamma-1}},\ u^e(x) = 0,\ p^e(x) = \left(\frac{1}{K}\right)^{\frac{1}{\gamma-1}}\left(\frac{\gamma-1}{\gamma}h^e(x)\right)^{\frac{\gamma}{\gamma-1}}.$$

  We can compute $U^e(x)$, and define $U_h^e(x) = P_h^+ U^e(x)$.

Decomposition into equilibrium and non-equilibrium parts

- Key idea: decompose U_h into the sum of a reference equilibrium state U_h^e and the remaining part U_h^r.
- $U_h^e(x)$? (Recover the (projected) equilibrium at the steady state)

  Let $h^e(x) = h(p_h(x_{j-\frac{1}{2}}), \rho_h(x_{j-\frac{1}{2}})) + \phi_h(x_{j-\frac{1}{2}}) - \phi(x)$. Recover $\rho^e(x)$ and $p^e(x)$ from $h^e(x)$. For the ideal gas law, we have the polytropic form

$$\rho^e(x) = \left(\frac{1}{K}\frac{\gamma-1}{\gamma}h^e(x)\right)^{\frac{1}{\gamma-1}},\ u^e(x) = 0,\ p^e(x) = \left(\frac{1}{K}\right)^{\frac{1}{\gamma-1}}\left(\frac{\gamma-1}{\gamma}h^e(x)\right)^{\frac{\gamma}{\gamma-1}}.$$

  We can compute $U^e(x)$, and define $U_h^e(x) = P_h^+ U^e(x)$.
- $U_h^r = U_h(x) - U_h^e(x)$.

  Note that both U_h^e and U_h^r are piecewise polynomials.
- At the polytropic steady state, $U_h^r(x) = 0$.

Decomposition into equilibrium and non-equilibrium parts

- Key idea: decompose U_h into the sum of a reference equilibrium state U_h^e and the remaining part U_h^r.

- $U_h^e(x)$? (Recover the (projected) equilibrium at the steady state)

  The same technique can be extended to the isothermal equilibrium state (Li-X, JCP 2018), or any given (family of) equilibrium solutions.

  What if the equilibrium is not known, i.e., we only know $f(U)_x = s(U, x)$? One could follow the idea† to solve the ODE to recover $U^e(x)$.

†C. Parés, C. Parés-Pulido, *Well-balanced high-order finite difference methods for systems of balance laws*, JCP 2020.

Well-balanced fluxes (Hydrostatic reconstruction)

- The hydrostatic reconstructed cell boundary values are defined by:

$$U^{*,\pm}_{j+\frac{1}{2}} = U^e\left(h(p_h(x_j),\rho_h(x_j)) + \phi_h(x_j) - \max(\phi^{\pm}_{h,j+\frac{1}{2}})\right) + (U^r_h)^{\pm}_{j+\frac{1}{2}},$$

  In the case of polytropic equilibrium, $U^{*,+}_{j+\frac{1}{2}} = U^{*,-}_{j+\frac{1}{2}}$.

- The left and right fluxes $\widehat{f}^l_{j+\frac{1}{2}}$ and $\widehat{f}^r_{j-\frac{1}{2}}$ are given by:

$$\begin{aligned}
\widehat{f}^l_{j+\frac{1}{2}} &= F(U^{*,-}_{j+\frac{1}{2}}, U^{*,+}_{j+\frac{1}{2}}) + f(U^-_{j+\frac{1}{2}}) - f(U^{*,-}_{j+\frac{1}{2}}),\\
\widehat{f}^r_{j-\frac{1}{2}} &= F(U^{*,-}_{j-\frac{1}{2}}, U^{*,+}_{j-\frac{1}{2}}) + f(U^+_{j-\frac{1}{2}}) - f(U^{*,+}_{j-\frac{1}{2}}).
\end{aligned}$$

Source term approximation

- For $-\int(\rho u)_h(\phi_h)_x v dx$, we apply the Gaussian quadrature rule directly.
- $-\rho_h(\phi_h)_x$ is linear with respect to ρ_h, we have

$$-\int \rho_h \phi_{h,x} v dx = -\int \rho_h^e (\phi_h)_x v dx - \int \rho_h^r (\phi_h)_x v dx,$$

which can be approximated by:

$$-\int \rho_h(\phi_h)_x v dx \approx p^{e,-}_{h,j+\frac{1}{2}} v(x^-_{j+\frac{1}{2}}) - p^{e,+}_{h,j-\frac{1}{2}} v(x^+_{j-\frac{1}{2}}) - \int_{I_j} p_h^e v_x \,\mathrm{d}x - \int_{I_j} \rho_h^r (\phi_h)_x v \,\mathrm{d}x,$$

using the fact that U_h^e is the equilibrium state.

Well-balanced methods for polytropic balance

$$\int_{I_j} \partial_t U^n v dx - \int_{I_j} f(U^n) \partial_x v dx + \widehat{f}^l_{j+\frac{1}{2}} v(x^-_{j+\frac{1}{2}}) - \widehat{f}^r_{j-\frac{1}{2}} v(x^+_{j-\frac{1}{2}}) = \int_{I_j} s(h^n, b) v dx,$$

Propoposition: The DG schemes described above maintain the equilibrium exactly.

Well-balanced methods for polytropic balance

$$\int_{I_j} \partial_t U^n v dx - \int_{I_j} f(U^n) \partial_x v dx + \widehat{f}^l_{j+\frac{1}{2}} v(x^-_{j+\frac{1}{2}}) - \widehat{f}^r_{j-\frac{1}{2}} v(x^+_{j-\frac{1}{2}}) = \int_{I_j} s(h^n, b) v dx,$$

Propoposition: The DG schemes described above maintain the equilibrium exactly.

Remarks

- If there is no gravitation field, i.e., $\phi_x = 0$, our well-balanced DG methods become the traditional DG methods.
- The first order version of our well-balanced methods reduces to the method in (Käppeli and Mishra, JCP 2014).

Multi-dimensional Euler equations on unstructured meshes

The same four components: (details skipped)

- Recovery of well-balanced states;
- Decomposition of the solutions into equilibrium and non-equilibrium parts;
- Numerical fluxes via hydrostatic reconstruction;
- Novel source term approximation;

Numerical results

- The third order finite element DG schemes are implemented, for the flux and the source terms.
- Time discretization is by the third order TVD Runge-Kutta method:

$$\begin{aligned} U^{(1)} &= U^n + \Delta t \mathcal{F}(U^n) \\ U^{(2)} &= \frac{3}{4}U^n + \frac{1}{4}\left(U^{(1)} + \Delta t \mathcal{F}(U^{(1)})\right) \\ U^{n+1} &= \frac{1}{3}U^n + \frac{2}{3}\left(U^{(2)} + \Delta t \mathcal{F}(U^{(2)})\right), \end{aligned}$$

  where $\mathcal{F}(U)$ is the spatial operator.
- The CFL number is taken as 0.18.

One dimensional polytropic equilibrium solution

- The gravitational force, with $g = \phi_x = 1$, acts in the negative x direction.
- Consider a polytropic equilibrium solution

$$\rho(x) = \left(\rho_0^{\gamma-1} - \frac{1}{K_0}\frac{\gamma-1}{\gamma}gx\right)^{\frac{1}{\gamma-1}}, \quad u(x) = 0, \quad p(x) = K_0\rho(x)^\gamma,$$

in the domain $[0, 2]$, with $\gamma = 5/3,\ \rho_0 = 1,\ p_0 = 1$ and $K_0 = p_0/\rho_0^\gamma$.

Table: L^1 errors for different precisions.

N	Precision	ρ	ρu	E
100	Single	1.01E-6	1.48E-7	8.27E-7
	Double	1.33E-15	1.55E-16	8.75E-16
200	Single	4.53E-6	5.24E-7	2.83E-7
	Double	3.34E-15	5.10E-15	2.67E-16

Perturbation of the equilibrium solution

Impose a small perturbation to the velocity state at the bottom

$$u(0,t) = 10^{-6}\sin(4\pi t)$$

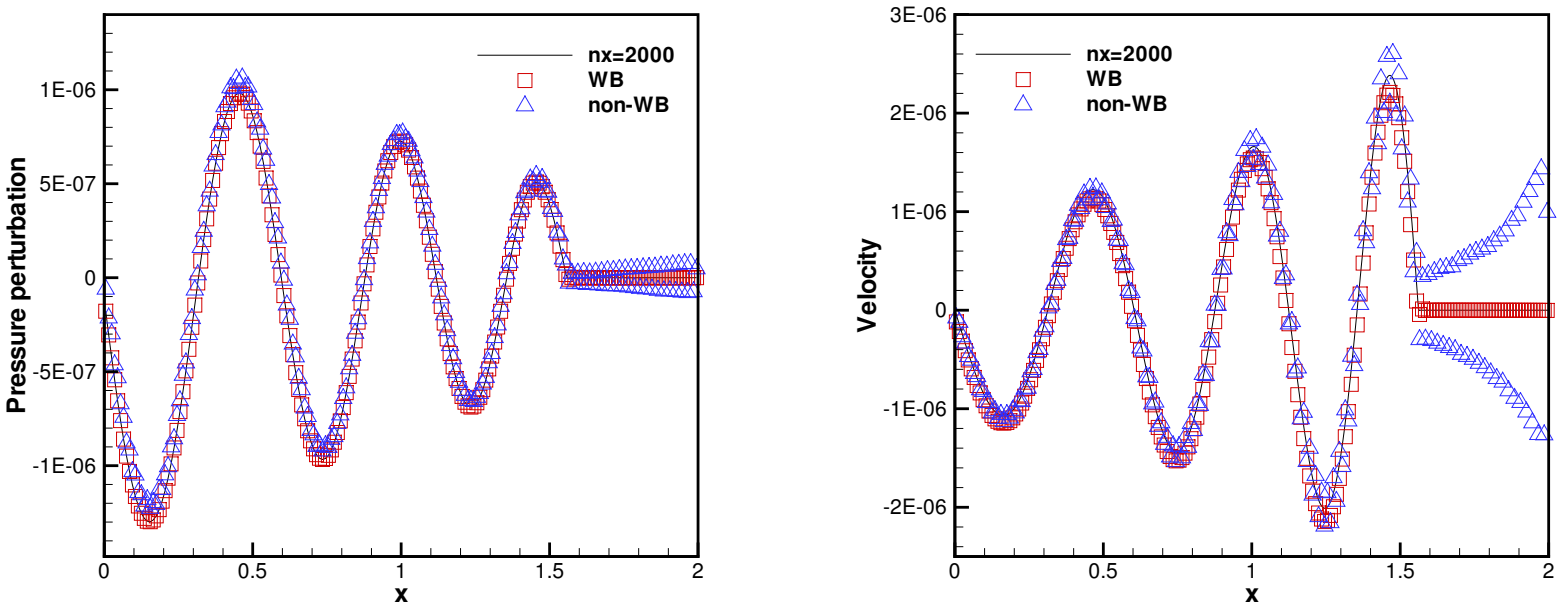

Figure: The pressure perturbations (left) and velocity (right) of a hydrostatic solution with small perturbation. The results of the well-balanced method vs. non-well-balanced method.

Perturbation of the equilibrium solution

Impose a large perturbation to the velocity state at the bottom

$$u(0,t) = 10^{-1}\sin(4\pi t)$$

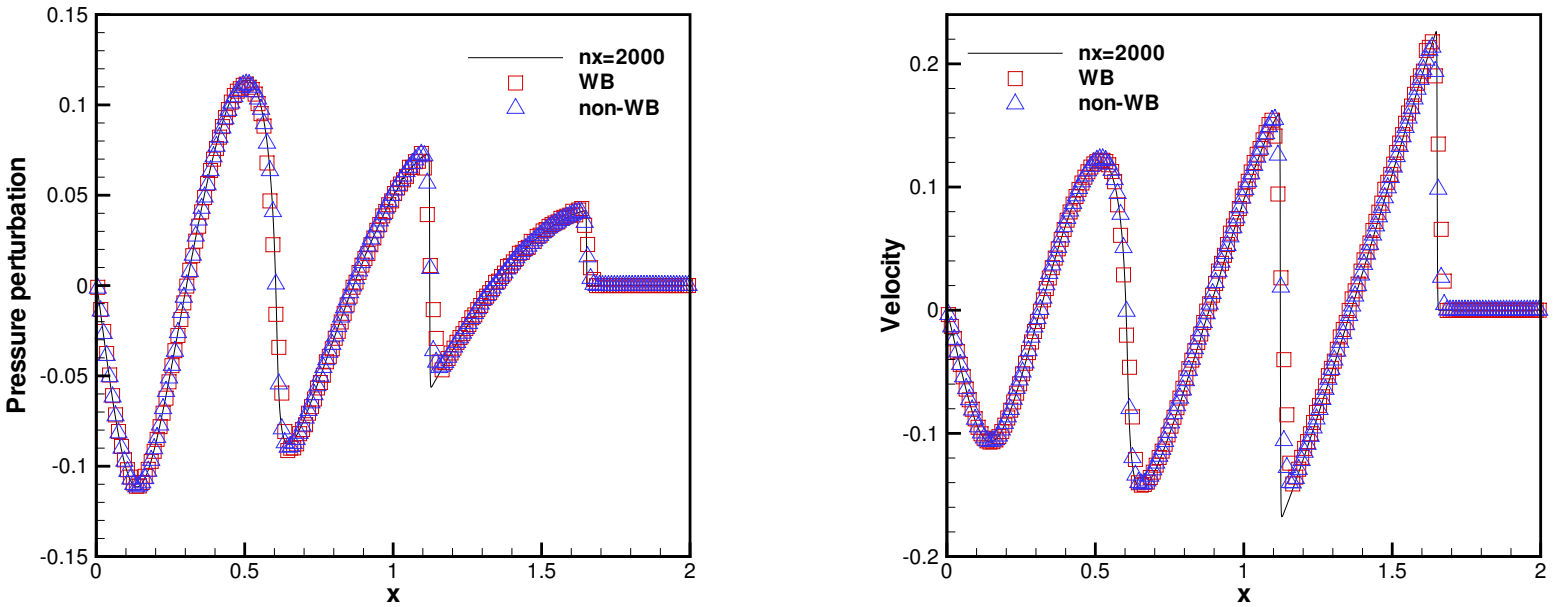

Figure: The pressure perturbations (left) and velocity (right) of a hydrostatic solution with large perturbation. The results of the well-balanced method vs. non-well-balanced method.

One dimensional isothermal equilibrium solution

- The gravitational force, with $g = \phi_x = 1$, acts in the negative x direction.
- Consider an isothermal equilibrium solution

$$\rho_0(x) = p_0(x) = \exp(-x), \qquad \text{and} \qquad u_0(x) = 0.$$

in the domain $[0, 1]$.

Table: L^1 errors for different precisions.

N	Precision	ρ	ρu	E
100	Single	2.38E-7	2.23E-7	4.55E-7
	Double	1.76E-15	1.77E-15	1.24E-15
200	Single	3.13E-7	2.34E-7	4.31E-7
	Double	2.99E-15	1.61E-15	1.84E-15

Perturbation of the equilibrium solution

Impose a small perturbation to the initial pressure state

$$p(x, t = 0) = p_0(x) + \eta \exp(-100(x - 0.5)^2),$$

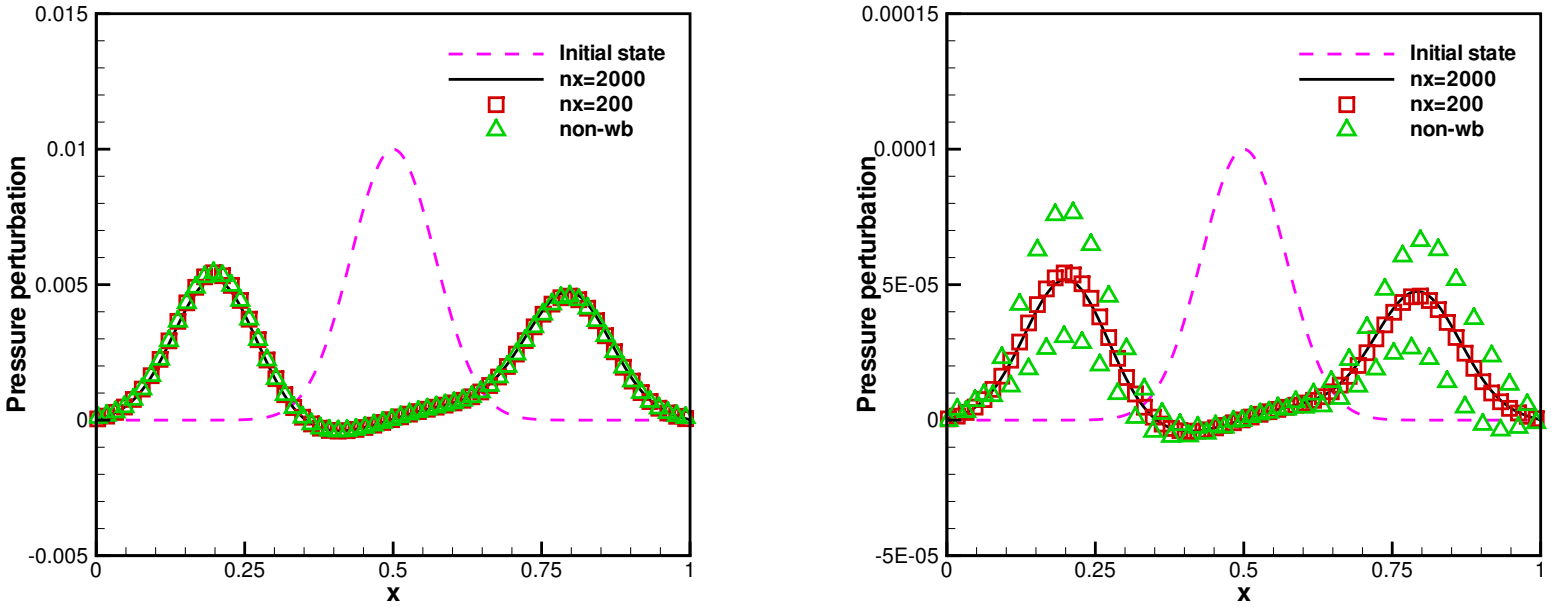

Figure: The pressure perturbation of a hydrostatic solution. The results of the well-balanced method vs. non-well-balanced method. Left: $\eta = 0.01$; Right: $\eta = 0.0001$.

One dimensional gas falling into a fixed external potential

- The gravitational potential has the form of a sine wave,

$$\phi(x) = -\phi_0 \frac{L}{2\pi} \sin \frac{2\pi x}{L},$$

  where L is the computational domain length and ϕ_0 is the amplitude.
- Consider an isothermal equilibrium solution

$$\rho = \rho_0 \exp\left(-\frac{\phi}{RT}\right), \qquad u = 0, \qquad p = RT\rho_0 \exp\left(-\frac{\phi}{RT}\right),$$

  with a constant temperature T.
- Add a small perturbation to the steady state:

$$\rho = \rho_0 \exp\left(-\frac{\phi}{RT}\right), \quad u = 0,$$

$$p = RT\rho_0 \exp\left(-\frac{\phi}{RT}\right) + 0.001 \exp\left(-10(x-32)^2\right).$$

- We run the simulation with 64 uniform cells for $1,000,000$ time steps.

One dimensional gas falling into a fixed external potential

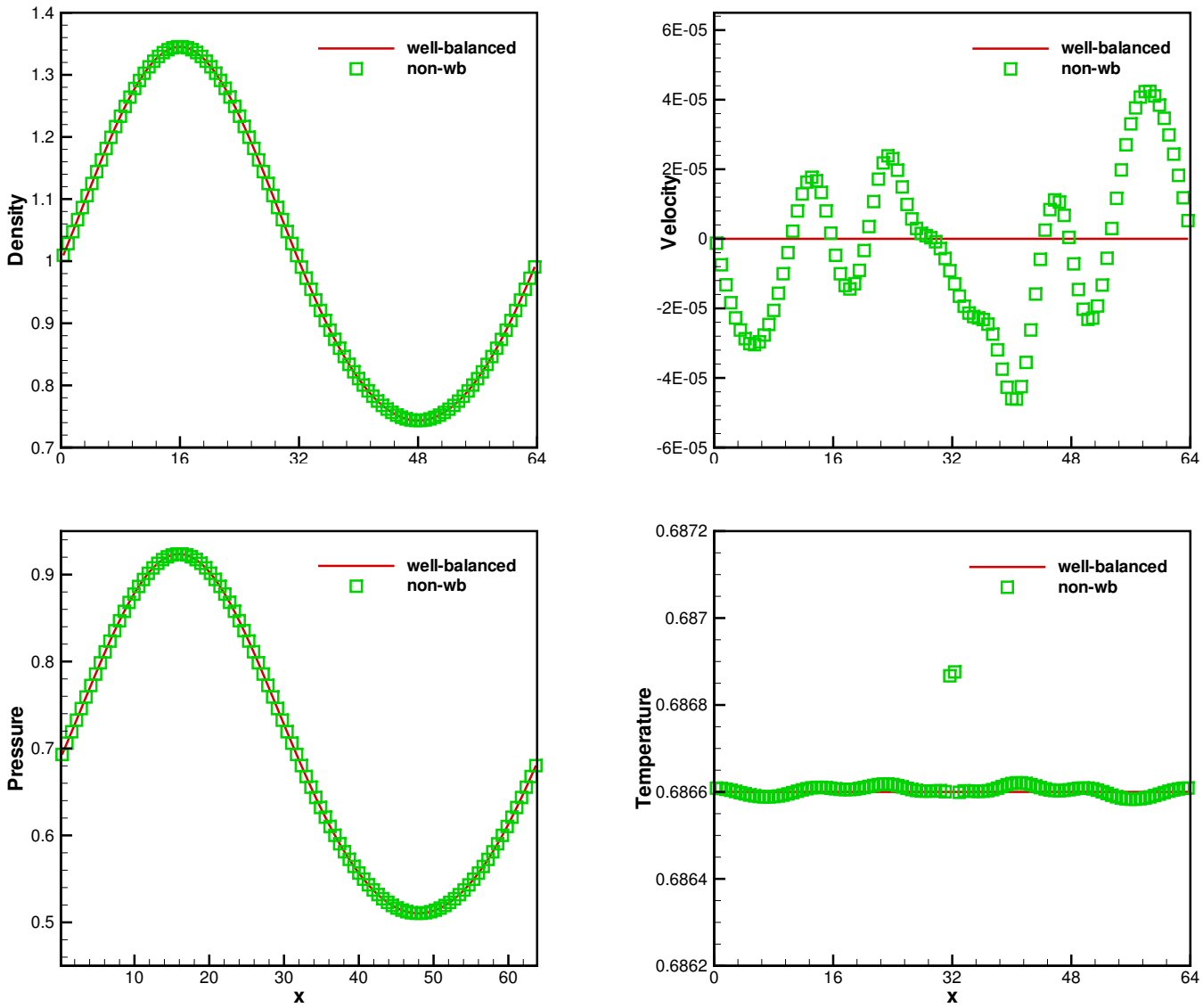

Figure: The numerical solutions of well-balanced method (solid line) and non-well-balanced method (square box, denoted by non-wb)

Two dimensional accuracy test

- Consider a linear gravitational field $\phi_x = \phi_y = 1$, in a computational domain $[0,\, 2] \times [0,\, 2]$.
- A time dependent exact solution

$$\begin{aligned}
&\rho(x, y, t) = 1 + 0.2 \sin(\pi(x + y - t(u_0 + v_0))),\\
&u(x, y, t) = u_0, \qquad\qquad v(x, y, t) = v_0,\\
&p(x, y, t) = t(u_0 + v_0) - x - y + 0.2\pi \cos(\pi(x + y - t(u_0 + v_0))).
\end{aligned}$$

- The exact solutions are used as the boundary condition. We compute up to $t = 0.1$.

Two dimensional accuracy test

Table: L^1 errors and numerical orders of accuracy for the example (the error of ρv is similar to ρu and is not listed here).

Cells	ρ		ρu		E	
	L^1 error	Order	L^1 error	Order	L^1 error	Order
8×8	1.20E-04		1.09E-04		2.84E-04	
16×16	1.19E-05	3.33	1.13E-05	3.27	3.18E-05	3.16
32×32	1.14E-06	3.39	1.17E-06	3.27	3.61E-06	3.14
64×64	1.35E-07	3.07	1.58E-07	2.89	4.10E-07	3.14
128×128	1.80E-08	2.91	2.15E-08	2.88	4.78E-08	3.10
256×256	2.41E-09	2.90	2.94E-09	2.87	5.93E-09	3.01

Two dimensional polytrope

- An adiabatic gaseous sphere held together by self-gravitation, modeled by the hydrostatic equilibrium

$$\frac{\mathrm{d}p}{\mathrm{d}r} = -\rho\frac{\mathrm{d}\phi}{\mathrm{d}r},$$

and Poisson's equation with $r = \sqrt{x^2 + y^2}$

$$\frac{1}{r^2}\frac{\mathrm{d}}{\mathrm{d}r}\left(r^2\frac{\mathrm{d}\phi}{\mathrm{d}r}\right) = 4\pi g\rho.$$

- Use the polytropic relation $p = K\rho^\gamma$, assume $\gamma = 2$ to obtain solutions:

$$\rho(r) = \rho_c\frac{\sin(\alpha r)}{\alpha r}, \quad p(r) = K\rho(r)^2, \tag{1}$$

with $\alpha = \sqrt{\frac{4\pi g}{2K}}$, and the gravitational potential

$$\phi(r) = -2K\rho_c\frac{\sin(\alpha r)}{\alpha r}. \tag{2}$$

The parameters $K = g = \rho_c = 1$ are used.

Small perturbation of the 2D polytrope

Consider a small Gaussian hump perturbations to the initial pressure state

$$p(r) = K\rho(r)^2 + A\exp(-100r^2),$$

where A is taken as 10^{-3}.

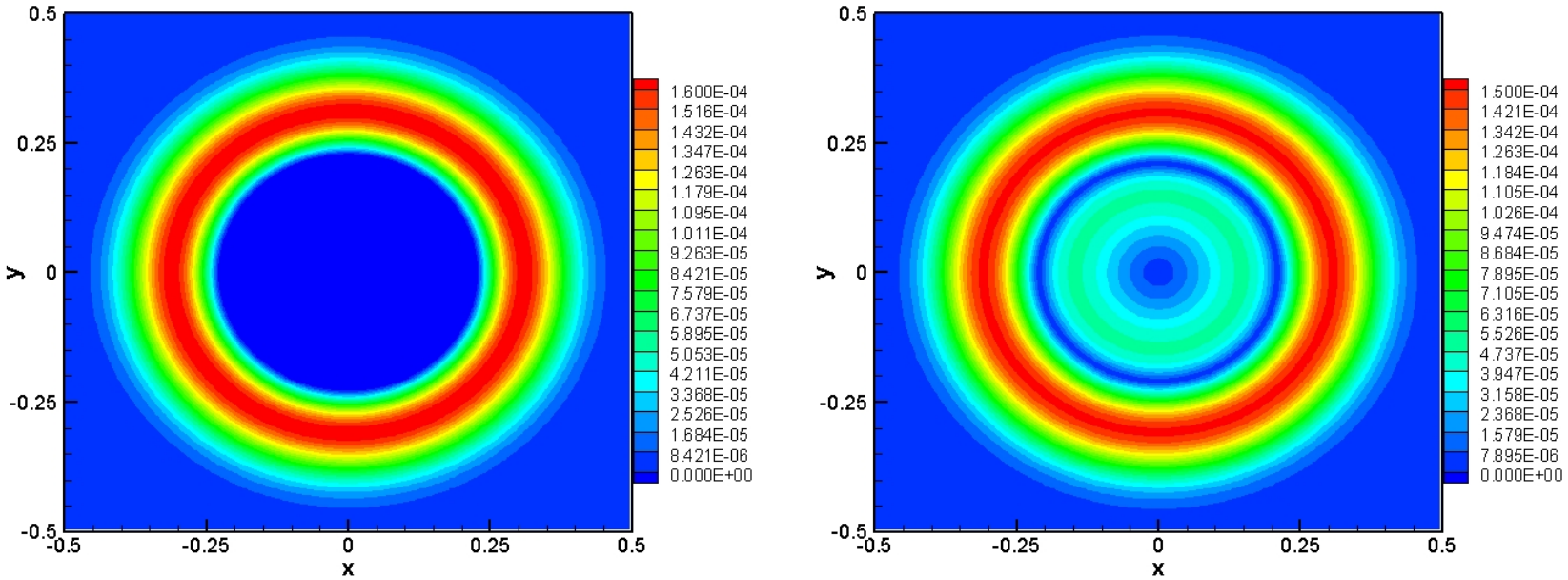

Figure: Well-balanced methods: The contours of the pressure and velocity perturbation of a two dimensional hydrostatic solution with 100×100 cells at $t = 0.2$. Left: pressure p. Right: velocity $\sqrt{u^2 + v^2}$.

Small perturbation of the 2D polytrope

Consider a small Gaussian hump perturbations to the initial pressure state

$$p(r) = K\rho(r)^2 + A\exp(-100r^2),$$

where A is taken as 10^{-3}.

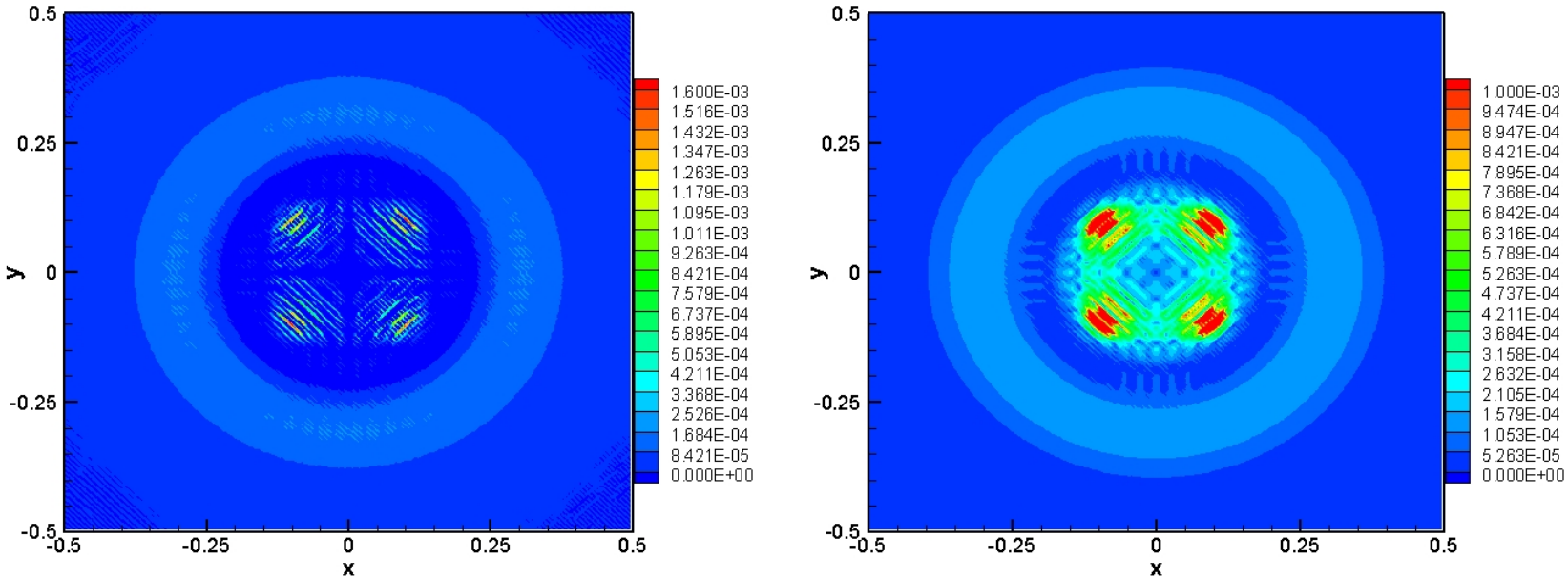

Figure: Non-well-balanced methods: The contours of the pressure and velocity perturbation of a two dimensional hydrostatic solution with 100×100 cells at $t = 0.2$. Left: pressure p. Right: velocity $\sqrt{u^2 + v^2}$. Notice the different contour range.

Small perturbation of the 2D equilibrium solution

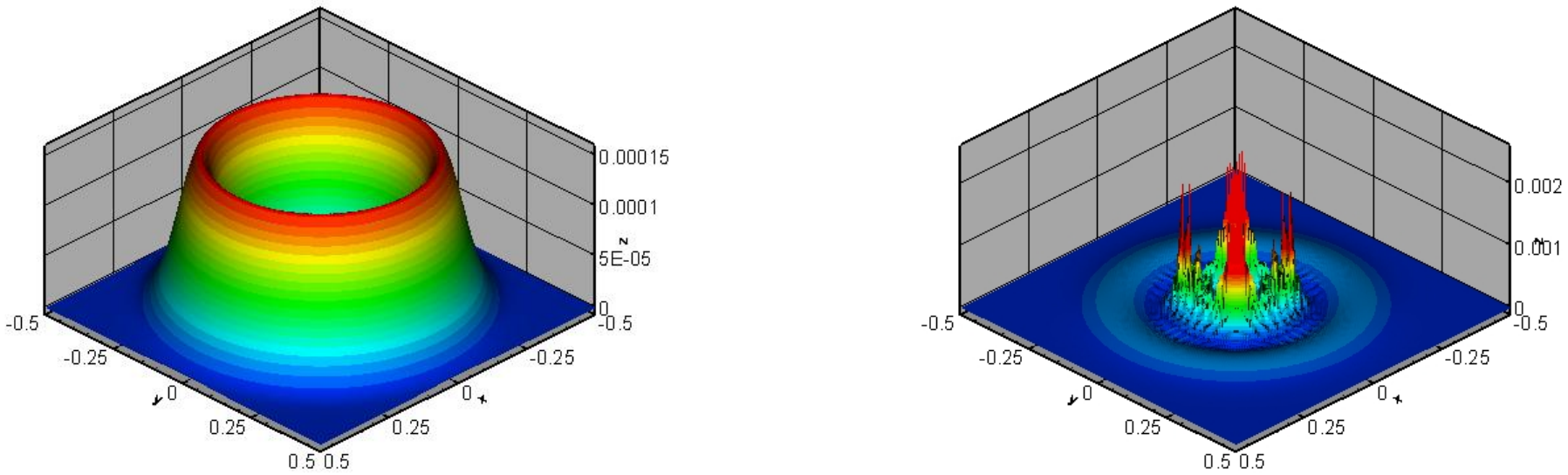

Figure: The 3D views of the velocity $\left(\sqrt{u^2+v^2}\right)$. Left: well-balanced methods; Right: non-well-balanced methods.

Two-dimensional Explosion Problem

- Linear gravitational field with $\phi_x = 0$, $\phi_y = g = 0.118$, an ideal gas ($\gamma = 1.4$)
- On the domain $[0, 3] \times [0, 3]$, initial conditions

$$
\begin{aligned}
&\rho(x, y, t = 0) = 1, \\
&u(x, y, t = 0) = 0, \\
&v(x, y, t = 0) = 0, \\
&p(x, y, t = 0) = 1 - gy + \begin{cases} 0.005, & \text{if } (x - 1.5)^2 + (y - 1.5)^2 < 0.01, \\ 0, & \text{otherwise.} \end{cases}
\end{aligned}
$$

- This test can also be viewed as a small perturbation of the steady state solution. But the underline steady state does not have the form of polytropic nor isothermal balance.

Two-dimensional Explosion Problem

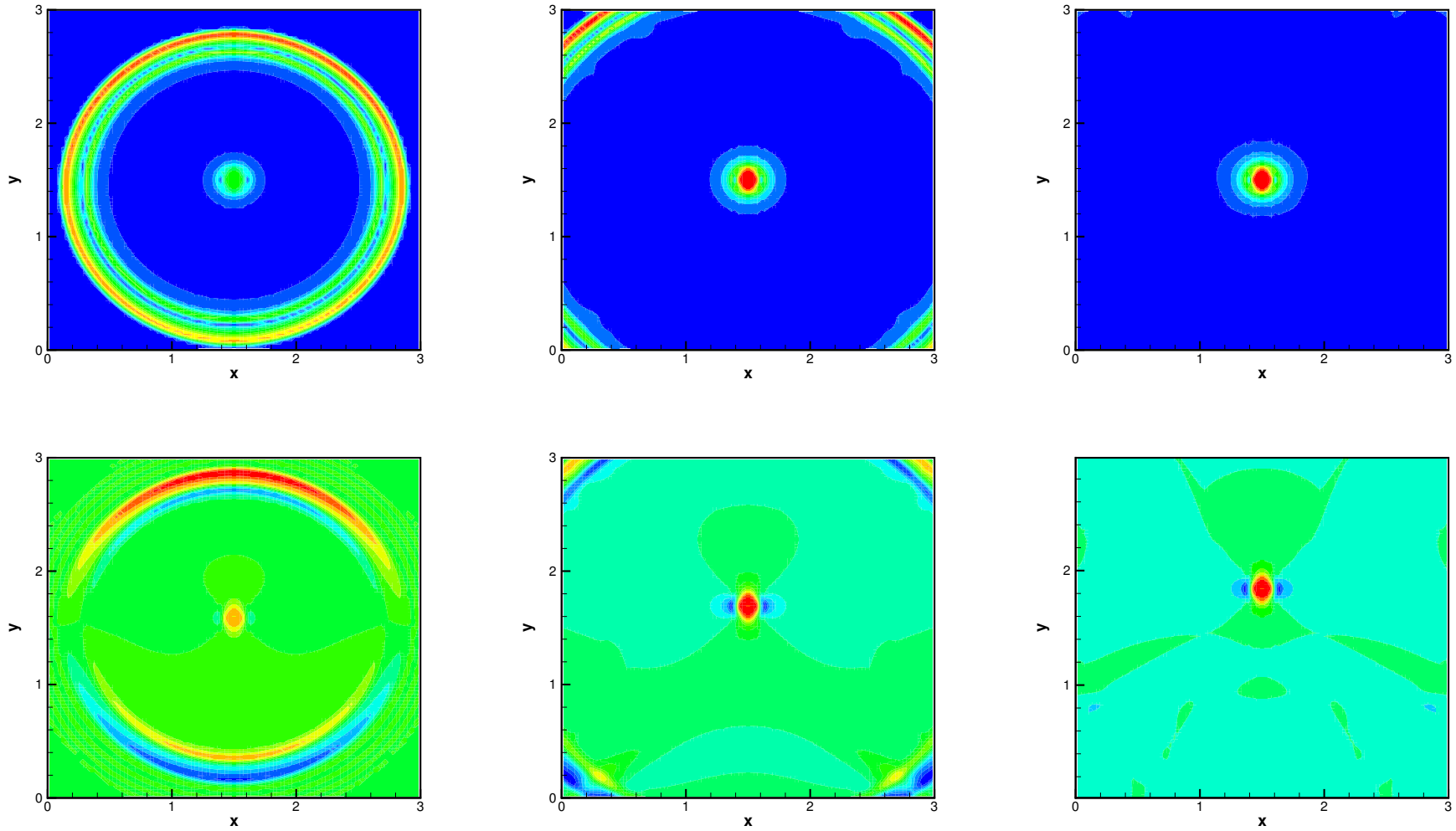

Figure: Velocity $\sqrt{u^2+v^2}$ at times $t = 1.2$ (left), $t = 1.8$ (middle) and $t = 2.4$ (right). Top: well-balanced. Bottom: non-well-balanced. Ten uniformly spaced contour lines from 0.2829 to 0.2838.

Positivity preserving (PP) methods

Existing work on PP DG methods for Euler equations

$$
\begin{aligned}
&\rho_t + \nabla \cdot (\rho \mathbf{u}) = 0, \\
&(\rho \mathbf{u})_t + \nabla \cdot (\rho \mathbf{u} \otimes \mathbf{u} + p \mathbf{I}_d) = -\rho \nabla \phi, \\
&E_t + \nabla \cdot ((E + p)\mathbf{u}) = -\rho \mathbf{u} \cdot \nabla \phi,
\end{aligned}
$$

- Density ρ and internal energy e should stay non-negative
- Many existing works available on PP methods for Euler equations, here we focus on Zhang-Shu JCP 2011 for Euler equations with source terms
- Define the set of physically admissible states

$$
G := \left\{ \mathbf{U} = (\rho, \mathbf{m}, E)^\top : \ \rho > 0, \ \mathcal{E}(\mathbf{U}) := \rho E - \frac{|\mathbf{m}|^2}{2} > 0 \right\},
$$

G is a convex set.

Positivity-preserving methods

- ρ and p should be non-negative. Unfortunately, there are negative ρ or p in our simulations when high order methods are used.

  Goal: maintain the non-negativity of ρ and p.

  Montone scheme (positivity) $\Rightarrow$ first order (Godunov's theorem)
  High order accuracy & positivity $\Rightarrow$ nontrivial.

Positivity-preserving methods

- ρ and p should be non-negative. Unfortunately, there are negative ρ or p in our simulations when high order methods are used.

  Goal: maintain the non-negativity of ρ and p.

  Montone scheme (positivity) $\Rightarrow$ first order (Godunov's theorem)
  High order accuracy & positivity $\Rightarrow$ nontrivial.

- One time step of traditional DG methods:

$$\boxed{\mathbf{U}_h^n(x)} \xrightarrow{\text{DG update}} \boxed{\mathbf{U}_h^{n+1}(x)}$$

Positivity-preserving methods

- ρ and p should be non-negative. Unfortunately, there are negative ρ or p in our simulations when high order methods are used.

  Goal: maintain the non-negativity of ρ and p.

  Montone scheme (positivity) $\Rightarrow$ first order (Godunov's theorem)
  High order accuracy & positivity $\Rightarrow$ nontrivial.

- One time step of traditional DG methods:

  $$\boxed{\mathbf{U}_h^n(x)} \xrightarrow{\text{DG update}} \boxed{\mathbf{U}_h^{n+1}(x)}$$

  But one can show:

  $$\boxed{\mathbf{U}_h^n(x) \in G} \xrightarrow{\text{DG update}} \boxed{\mathbf{U}_h^{n+1}(x) \in G}$$ is at most second order

Positivity-preserving methods

- ρ and p should be non-negative. Unfortunately, there are negative ρ or p in our simulations when high order methods are used.

  Goal: maintain the non-negativity of ρ and p.

  Montone scheme (positivity) $\Rightarrow$ first order (Godunov's theorem)
  High order accuracy & positivity $\Rightarrow$ nontrivial.

- One time step of traditional DG methods:

$$\boxed{\mathbf{U}_h^n(x)} \xrightarrow{\text{DG update}} \boxed{\mathbf{U}_h^{n+1}(x)}$$

  But one can show:

$$\boxed{\mathbf{U}_h^n(x) \in G} \xrightarrow{\text{DG update}} \boxed{\mathbf{U}_h^{n+1}(x) \in G}$$ is at most second order

  To achieve high order & positivity

$$\boxed{\mathbf{U}_h^n(x) \in G} \xrightarrow[step\,1]{\text{DG update}} \boxed{\mathbf{U}_h^{n+1}(x) \text{ with } \overline{\mathbf{U}}_{h,j}^{n+1} \in G} \xrightarrow[step\,2]{\text{limiter}} \boxed{\mathbf{U}_h^{n+1}(x) \in G}$$

PP methods for Euler equations by Zhang-Shu JCP 2011

(Without source term) to achieve high order & positivity

$$\boxed{\mathbf{U}_h^n(x) \in G} \xrightarrow[step\,1]{\text{DG update}} \boxed{\mathbf{U}_h^{n+1}(x) \text{ with } \overline{\mathbf{U}}_{h,j}^{n+1} \in G} \xrightarrow[step\,2]{\text{limiter}} \boxed{\mathbf{U}_h^{n+1}(x) \in G}$$

PP methods for Euler equations by Zhang-Shu JCP 2011

(Without source term) to achieve high order & positivity

$$\boxed{\mathbf{U}_h^n(x) \in G} \xrightarrow[step\,1]{\text{DG update}} \boxed{\mathbf{U}_h^{n+1}(x) \text{ with } \overline{\mathbf{U}}_{h,j}^{n+1} \in G} \xrightarrow[step\,2]{\text{limiter}} \boxed{\mathbf{U}_h^{n+1}(x) \in G}$$

- Step 1: proven analytically under the CFL condition $\alpha \Delta t / \Delta x \le \widehat{w}_1$
- Step 2: obtained via a simple PP limiter on density ρ

$$\widetilde{\rho}_j^n(x) = \theta\left(\rho_j^n(x) - \overline{\rho}_j^n\right) + \overline{\rho}_j^n, \qquad \theta = \min\left\{1, \frac{\overline{\rho}_j^n}{\overline{\rho}_j^n - m_j}\right\},$$

with

$$m_j = \min_{x \in I_j} \rho_j^n(x).$$

Similar limiter can be applied on the internal energy e (with new θ)

This limiter does not affect the high order accuracy and mass conservation.

PP methods for Euler equations by Zhang-Shu JCP 2011

(With source term $s(\mathbf{U}, x)$) to achieve high order & positivity

$$\boxed{\mathbf{U}_h^n(x) \in G} \xrightarrow[step\,1]{\text{DG update}} \boxed{\mathbf{U}_h^{n+1}(x) \text{ with } \overline{\mathbf{U}}_{h,j}^{n+1} \in G} \xrightarrow[step\,2]{\text{limiter}} \boxed{\mathbf{U}_h^{n+1}(x) \in G}$$

- Step 1: proven analytically under the CFL condition

$$\alpha \Delta t / \Delta x \le \widehat{w}_1 / 2, \qquad \text{and} \qquad \Delta t \le A_s(\mathbf{U_h}, x),$$

where $\Delta t \le A_s(\mathbf{U_h}, x)$ is chosen such that $\mathbf{U} + 2\Delta t s(\mathbf{U}, x) \in G$.

When the gravitational source $-\rho\phi_x$ is considered, the extra CFL condition is:

$$\Delta t \le \frac{\sqrt{2e}}{\phi_x},$$

- Step 2: SAME PP limiter.

PP well-balanced methods (step 1)

Combining these PP techniques with the first well-balanced methods

PP result

Assume that $\overline{\mathbf{U}}_{h,j} \in G$ and $\mathbf{U}_h(\widehat{x}_j^{(\nu)}) \in G$, $1 \le \nu \le L$, $\forall j$. Then under the CFL-type condition

$$\Delta t \left\{ \frac{\alpha_{j+\frac{1}{2}} \rho^{e,\max}_{j+\frac{1}{2}}}{\Delta x \widehat{w}_1 \rho_h^e(x^-_{j+\frac{1}{2}})} \left[\frac{\beta_{j+\frac{1}{2}}}{\beta_h(x^-_{j+\frac{1}{2}})} + \left(\frac{\beta_{j+\frac{1}{2}}}{\beta_h(x^-_{j+\frac{1}{2}})} - 1 \right) \frac{|u^-_{j+\frac{1}{2}}|^2}{2e^-_{j+\frac{1}{2}}} \right] + a_j^{\max} + \overline{a}_j \right\} \le 1$$

with $\beta_h = p_h/\rho_h$, $\beta_{j+\frac{1}{2}} = \max(\beta_h(x^-_{j+\frac{1}{2}}), \beta_h(x^+_{j+\frac{1}{2}}))$,

$$a_j^{\max} := \max_{1\le\mu\le N} \left\{ \frac{|(p_h^e)_x(x_j^{(\mu)}|)}{\rho_h^e(x_j^{(\mu)})\sqrt{2e_h(x_j^{(\mu)})}} \right\}, \quad \overline{a}_j := \frac{|p_h^e(x^+_{j+\frac{1}{2}}) - p_h^e(x^-_{j-\frac{1}{2}})|}{\Delta x \overline{(\rho_h^e)}_j \sqrt{2\overline{e}_j}},$$

one has

$$\overline{\mathbf{U}}_j + \Delta t \mathbf{L}_j(\mathbf{U}_h) \in G, \quad \forall j.$$

Restrictive CFL condition due to the modification of the numerical viscosity in the well-balanced LF flux

Modification of the well-balanced numerical fluxes

The HLLC numerical flux defined by

$$\mathbf{F}^{hllc}(\mathbf{U}_L, \mathbf{U}_R) = \begin{cases} \mathbf{F}(\mathbf{U}_L), & \text{if } 0 \le S_L, \\ \mathbf{F}_{*L}, & \text{if } S_L \le 0 \le S_*, \\ \mathbf{F}_{*R}, & \text{if } S_* \le 0 \le S_R, \\ \mathbf{F}(\mathbf{U}_R), & \text{if } 0 \ge S_R, \end{cases}$$

has the following contact property and positivity-preserving property:

- For any two states $\mathbf{U}_L = (\rho_L, 0, p/(\gamma-1))^\top$ and $\mathbf{U}_R = (\rho_R, 0, p/(\gamma-1))^\top$,

  $$\mathbf{F}^{hllc}(\mathbf{U}_L, \mathbf{U}_R) = (0, p, 0)^\top.$$

  Shown in Chandrashekar-Klingenberg SISC 2015

- Let $\mathcal{R}(x/t, \mathbf{U}_L, \mathbf{U}_R)$ be the approximate HLLC solution of the Riemann problem between the states $\mathbf{U}_L$ and $\mathbf{U}_R$, Then, $\mathcal{R}(x/t, \mathbf{U}_L, \mathbf{U}_R) \in G$, provided that $\mathbf{U}_L$ and $\mathbf{U}_R \in G$.

Modification of the well-balanced numerical fluxes

Modified well-balanced numerical fluxes:

$$\widehat{\mathbf{F}}_{j+\frac{1}{2}} = \mathbf{F}^{hllc}\left(\frac{p^{e,\star}_{j+\frac{1}{2}}}{p^e_h(x^-_{j+\frac{1}{2}})}\mathbf{U}^-_{j+\frac{1}{2}}, \frac{p^{e,\star}_{j+\frac{1}{2}}}{p^e_h(x^+_{j+\frac{1}{2}})}\mathbf{U}^+_{j+\frac{1}{2}}\right),$$

where $\mathbf{U}^{\pm}_{j+\frac{1}{2}} := \mathbf{U}_h(x^{\pm}_{j+\frac{1}{2}})$, and $p^{e,\star}_{j+\frac{1}{2}} = \max\left\{p^e_h(x^-_{j+\frac{1}{2}}), p^e_h(x^+_{j+\frac{1}{2}})\right\}$.

PP result (step 1 only)

Assume that $\overline{\mathbf{U}}_{h,j} \in G$ and $\mathbf{U}_h(\widehat{x}^{(\nu)}_j) \in G$, $1 \le \nu \le L$, $\forall j$. Then under the CFL-type condition

$$\Delta t\left\{\frac{2p^{e,\star}_{j\pm\frac{1}{2}}}{\Delta x\widehat{\omega}_1 p^e_h(x^{\mp}_{j\pm\frac{1}{2}})}\alpha_\infty + a^{\max}_j + \overline{a}_j\right\} \le 1, \quad \forall j,$$

with $\alpha_\infty := \max \alpha(\mathbf{U}^{\pm}_{j\pm\frac{1}{2}})$ and

$$a^{\max}_j := \max_{1\le\mu\le N}\left\{\frac{|(p^e_h)_x(x^{(\mu)}_j)|}{\rho^e_h(x^{(\mu)}_j)\sqrt{2e_h(x^{(\mu)}_j)}}\right\}, \quad \overline{a}_j := \frac{|p^e_h(x^+_{j+\frac{1}{2}}) - p^e_h(x^-_{j-\frac{1}{2}})|}{\Delta x\overline{(\rho^e_h)}_j\sqrt{2\overline{e}_j}},$$

one has

$$\overline{\mathbf{U}}_j + \Delta t\mathbf{L}_j(\mathbf{U}_h) \in G, \quad \forall j.$$

PP well-balanced methods for Euler equations with gravity

$\boxed{\mathbf{U}_h^n(x) \in G} \xrightarrow[step\,1]{\text{DG update}} \boxed{\mathbf{U}_h^{n+1}(x) \text{ with } \overline{\mathbf{U}}_{h,j}^{n+1} \in G} \xrightarrow[step\,2]{\text{limiter}} \boxed{\mathbf{U}_h^{n+1}(x) \in G}$

- Step 1: proven analytically under suitable CFL condition
- Step 2: obtained via a simple PP limiter on density ρ

$$\widetilde{\rho}_j^n(x) = \theta\left(\rho_j^n(x) - \overline{\rho}_j^n\right) + \overline{\rho}_j^n, \qquad \theta = \min\left\{1, \frac{\overline{\rho}_j^n}{\overline{\rho}_j^n - m_j}\right\},$$

with

$$m_j = \min_{x \in I_j} \rho_j^n(x).$$

Similar limiter can be applied on the internal energy e (with new θ)

- Similar conclusion can be obtained for the second approach based on hydrostatic reconstruction.

Leblanc problem in linear gravitational field

- A linear potential $\phi(x) = x$ with the initial condition

$$(\rho, u, p)(x, 0) = \begin{cases} (2, 0, 10^9), & x < 5, \\ (10^{-3}, 0, 1), & x > 5. \end{cases}$$

- The computational domain is taken as $[0, 10]$ with reflection boundary conditions at $x = 0$ and $x = 10$.
- This problem is highly challenging due to the presence of the strong jumps in the initial density and pressure.
- As the exact solution contains strong discontinuities, the WENO limiter is implemented right before the PP limiting procedure

Leblanc problem in linear gravitational field

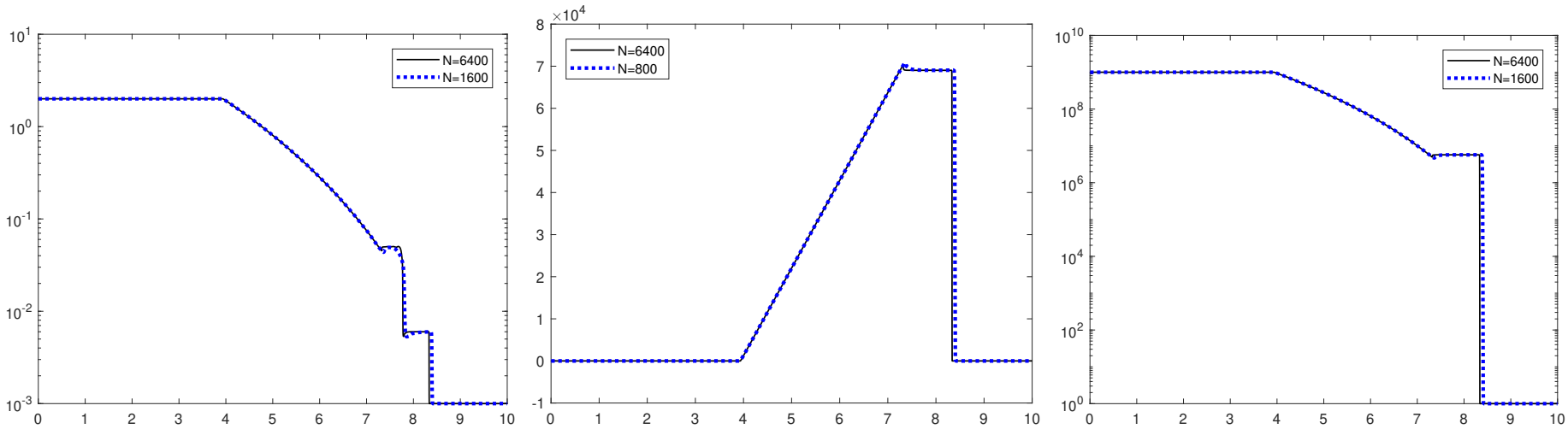

Figure: The log plot of density (left), the velocity (middle) and the log plot of pressure (right) for the extended Leblanc problem at $t = 0.00004$ obtained by the positivity-preserving WB scheme with 1600 and 6400 cells.

Two-dimensional blast problem

- The computational domain is taken as $[-0.5, 0.5]^2$.
- Consider the gravitational field

$$\phi(r) = -2K_0\rho_c \frac{\sin(\alpha r)}{\alpha r},$$

where $\alpha = \sqrt{2\pi g/K_0}$ with $K_0 = g = \rho_c = 1$, and $r := \sqrt{x^2 + y^2}$ denotes the radial variable.

- The initial data is obtained by adding a huge jump to the pressure term of the equilibrium

$$\rho(r) = \rho_c \frac{\sin(\alpha r)}{\alpha r}, \quad u(r) = v(r) = 0, \quad p(r,0) = K_0\rho(r)^2 + \begin{cases} 100, & r < 0.1, \\ 0, & r \geq 0.1. \end{cases}$$

We set the parameters $K_0 = g = 1$, $\gamma = 2$ and $\rho_c = 0.01$ so that low pressure and low density appear in the solution.

- In this extreme test, it is necessary to use the positivity-preserving limiting technique, otherwise we observe that the DG code would start to produce negative numerical pressure at $t \approx 0.00267$.

Two-dimensional blast problem

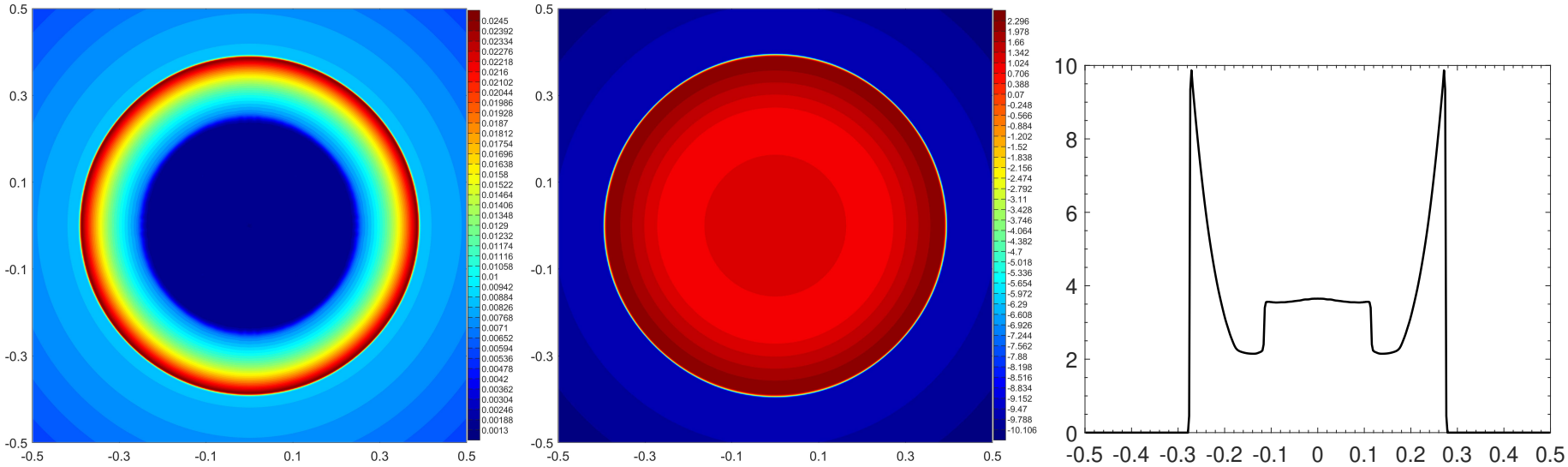

Figure: The contour plots of the density ρ (left) and the pressure logarithm $\log(p)$ (middle) at $t = 0.005$, and the plot of p (right) along the line $y = x$ within the *scaled* interval $[-0.5, 0.5]$.

Rising thermal bubble

- A benchmark test for atmospheric flows which simulates the dynamics of a warm bubble.
- The domain is $[0, 1000] \times [0, 1000]\ \mathrm{m}^2$, with inviscid wall boundary conditions.
- The gravitational field is linear with $\phi_x = 0$ and $\phi_y = g = 9.8\ \mathrm{m/s}^2$.
- Consider a stratified atmosphere, with zero velocity $\mathbf{u} = \mathbf{0}$, a constant potential temperature $\Theta = T_0 = 300\ \mathrm{K}$, and Exner pressure $\Pi = 1 - \frac{(\gamma-1)gy}{\gamma R T_0}$, where $R = 287.058\ \mathrm{J/kg\ K}$ is the gas constant.

  Initially, the warm bubble is added as a potential temperature perturbation to the hydrostatic balance,

$$\Delta\Theta(x, y, t = 0) = \begin{cases} 0, & r > r_c \\ \frac{\theta_c}{2}\left(1 + \cos(\pi r / r_c)\right), & r \le r_c, \end{cases}, \quad r = \sqrt{(x - x_c)^2 + (y - y_c)^2},$$

  where $\theta_c = 0.5\ \mathrm{K}$, $(x_c, y_c) = (500, 350)\ \mathrm{m}$, and $r_c = 250\ \mathrm{m}$.
- The initial circular bubble is deformed to a mushroomlike cloud.

Rising thermal bubble

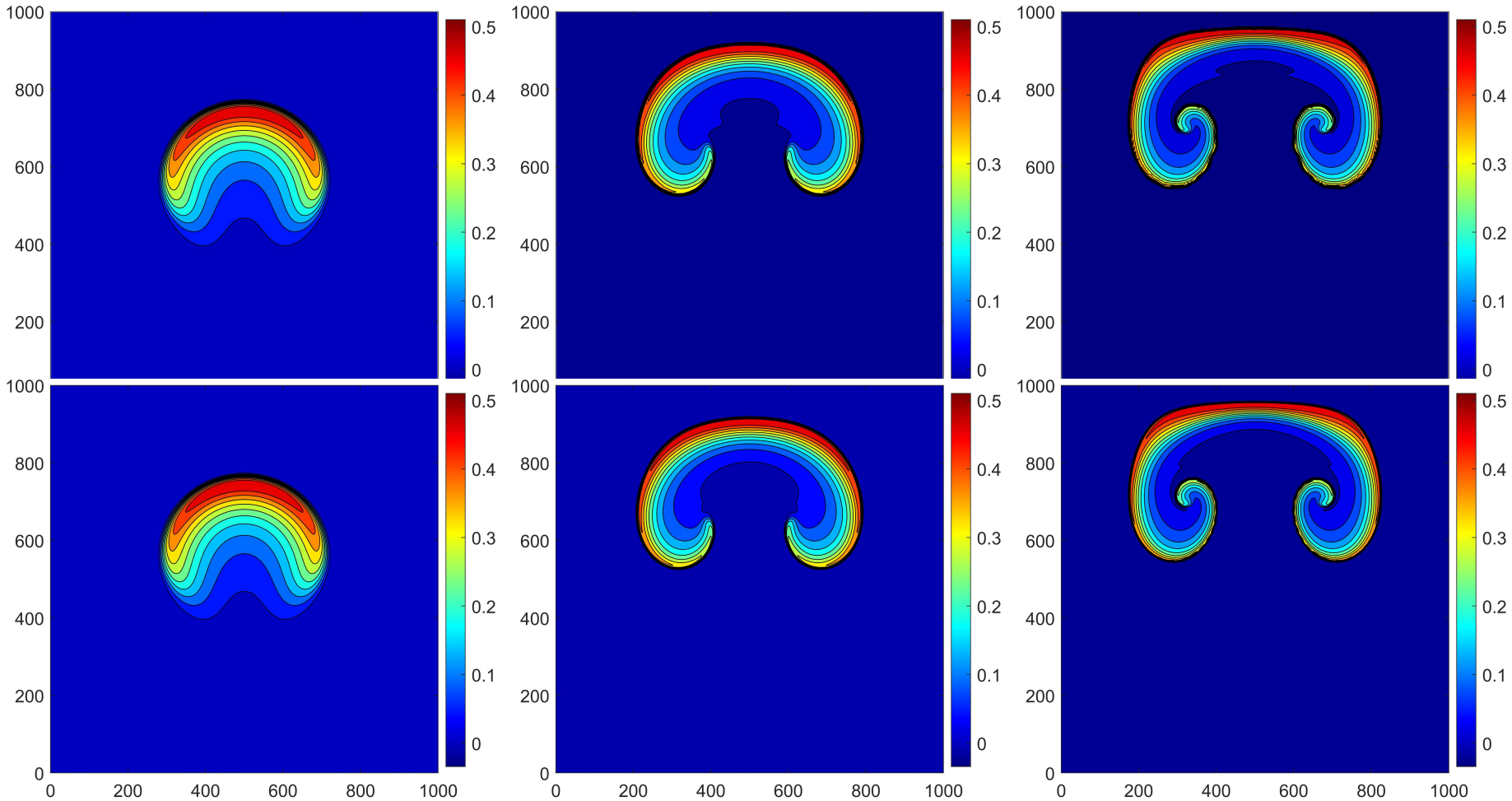

Figure: The contour plots of potential temperature perturbation $\Delta\Theta$ at $t = 400$ s (left), $t = 600$ s (middle), and $t = 700$ s (right), respectively, computed by our fifth-order DG method. 10 equally spaced contour lines are displayed. Top: mesh of 100×100 cells; bottom: mesh of 200×200 cells.

Triangular meshes

Multi-dimensional Euler equations

- The Euler equations with a static gravitational field are

$$\begin{aligned}
&\rho_t + \nabla \cdot (\rho \mathbf{u}) = 0, \\
&(\rho \mathbf{u})_t + \nabla \cdot (\rho \mathbf{u} \otimes \mathbf{u} + p \mathbf{I}_d) = -\rho \nabla \phi, \\
&E_t + \nabla \cdot ((E + p)\mathbf{u}) = -\rho \mathbf{u} \cdot \nabla \phi,
\end{aligned}$$

- Consider the unstructured meshes for multi-dimensional problem.

- The well-balanced and positivity-preserving methods can be extended to unstructured meshes (with some edits).

Inertia-gravity waves

- A two-dimensional benchmark for atmospheric models that involves the evolution of a potential temperature perturbation.
- The gravitational field of this problem is linear with $\phi_x = 0$ and $\phi_y = g = 9.8$.
- The initial flow is a perturbation added to a stratified atmosphere in hydrostatic balanced background

$$\rho(x,y) = \frac{p_0}{R\theta(x,y)}\left(1 + \frac{(\gamma-1)g^2}{\gamma R T_0 \mathcal{N}^2}(\exp(-\frac{\mathcal{N}^2}{g}y) - 1)\right)^{\frac{1}{\gamma-1}},$$
$$u(x,y) = 20, \qquad v(x,y) = 0,$$
$$p(x,y) = p_0\left(1 + \frac{(\gamma-1)g^2}{\gamma R T_0 \mathcal{N}^2}(\exp(-\frac{\mathcal{N}^2}{g}y) - 1)\right)^{\frac{\gamma}{\gamma-1}},$$

  where the reference pressure and temperature at $y = 0$ are $p_0 = 10^5$ and $T_0 = 300$, $\mathcal{N} = 0.01$, $R = 287.058$ and $\gamma = 1.4$.

- The potential temperature θ takes the form

$$\theta(x,y) = \theta_0 + \Delta\theta(x,y),$$

  where $\theta_0 = T_0 \exp(\frac{\mathcal{N}^2}{g}y)$, $\Delta\theta(x,y) = \theta_c \sin(\frac{\pi y}{h_c})\big(1 + (\frac{x-x_c}{a_c})^2\big)^{-1}$, $\theta_c = 0.01$, $h_c = 10000$, $a_c = 5000$, $x_c = 100000$.

Inertia-gravity waves

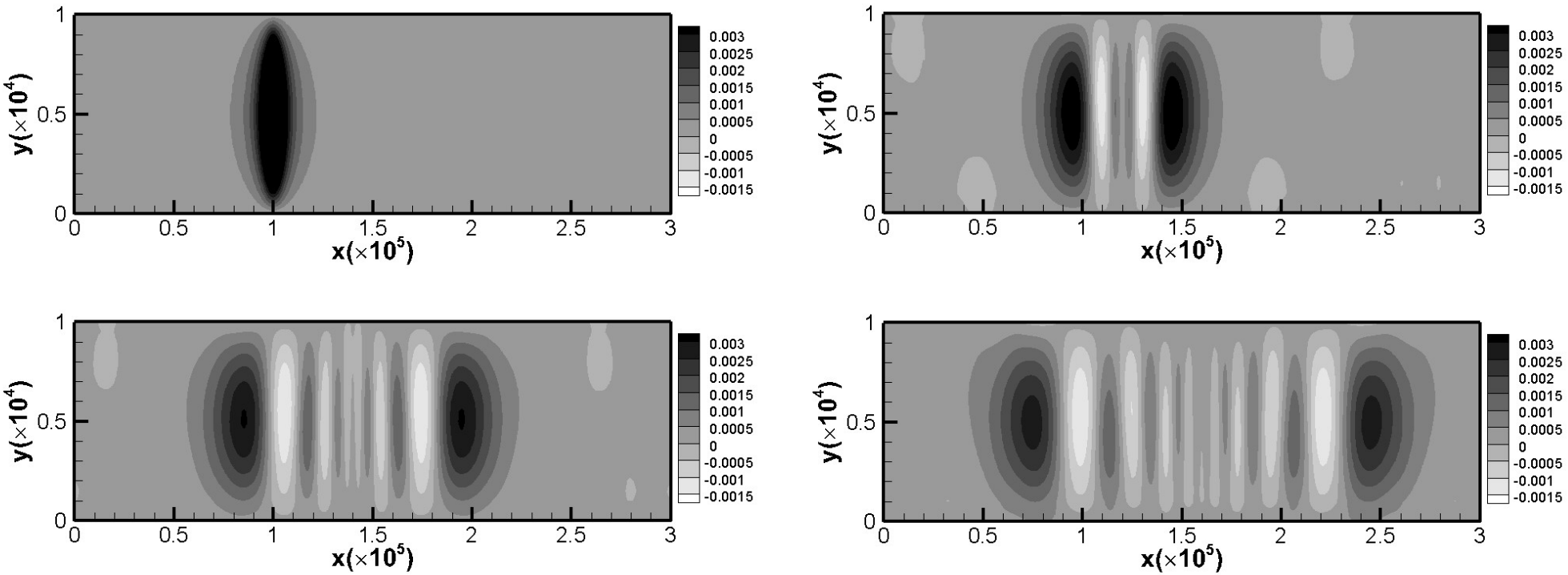

Figure: Potential temperature perturbation contour plots at time $T = 0$, 1000, 2000, 3000.

A shock wave diffracts at a convex corner

- We study a Mach 10 shock diffracting at a 120° convex corner.
- The initial condition is a pure right moving shock with Mach 10, initially located at the boundary $x = 3.4$ and $6 \leq y \leq 11$, moving into an undisturbed air ahead of the shock with

$$\phi(x, y) = 0.01x, \quad \rho(x, y) = 1.4, \quad \boldsymbol{m}(x, y) = 0, \quad p(x, y) = 1.0476 - \phi(x, y).$$

  The boundary conditions are inflow at $x = 3.4, 6 \leq y \leq 11$; outflow at $x = 13.6, 0 \leq y \leq 11$ and $y = 0, 0 \leq x \leq 13.6$ and $y = 11, 3.4 \leq x \leq 13.6$; reflective at other boundaries.

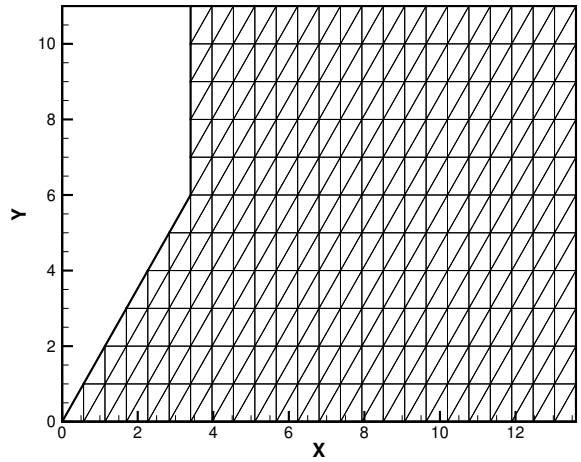

A shock wave diffracts at a convex corner

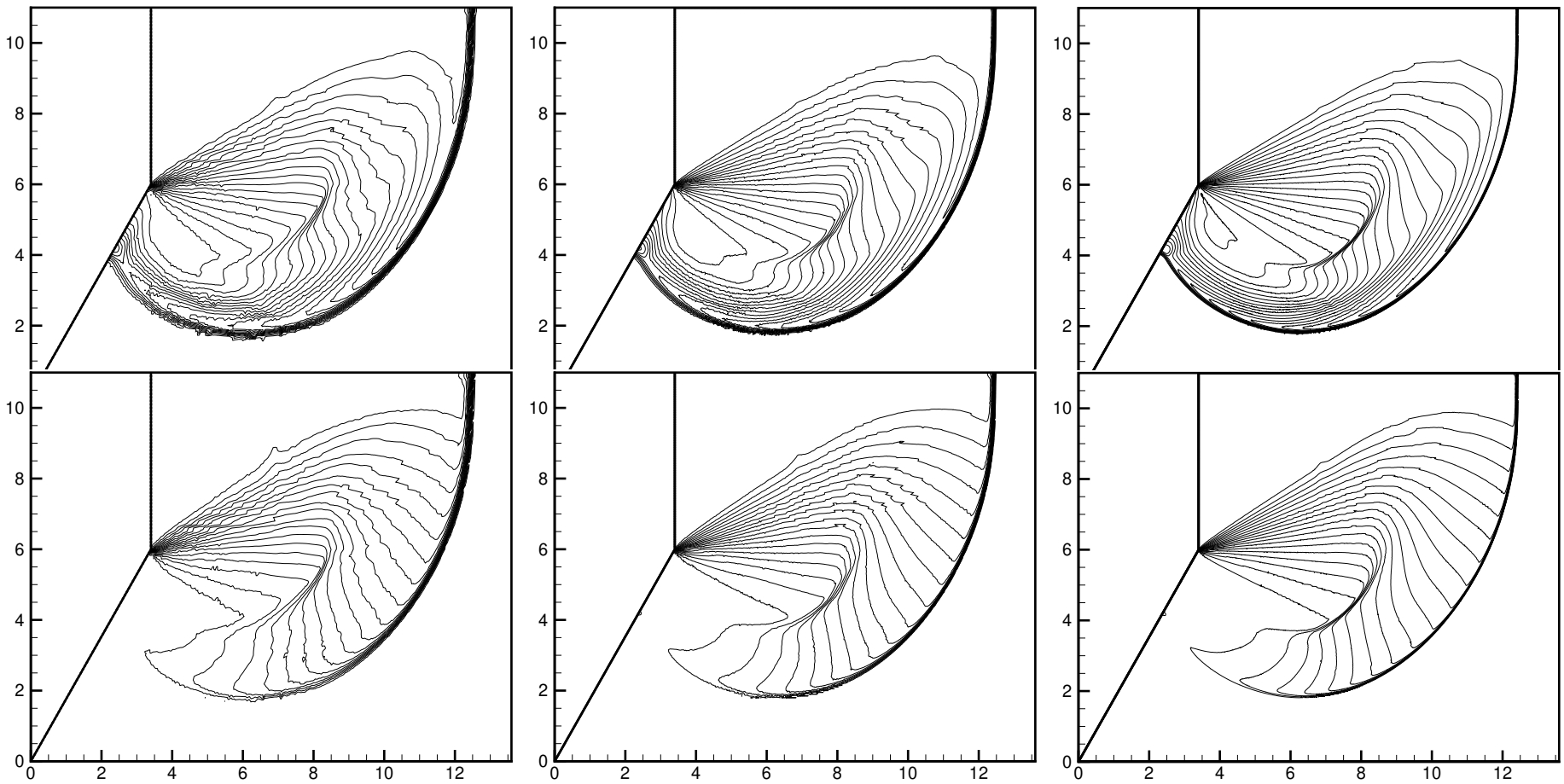

Figure: 20 uniform contour plots of density (top) and pressure (bottom) at $T = 0.9$. Top: mesh size $17/300$; Mid: mesh size $17/600$; Bottom: mesh size $17/1200$.

SWEs with a non-flat bottom topography

$$\begin{cases} h_t + (hu)_x = 0 \\ (hu)_t + \left(hu^2 + \frac{1}{2} g h^2 \right)_x = -ghb_x \end{cases}$$

- h : water height; u : velocity;
  b : bottom topography; g : gravitational constant.

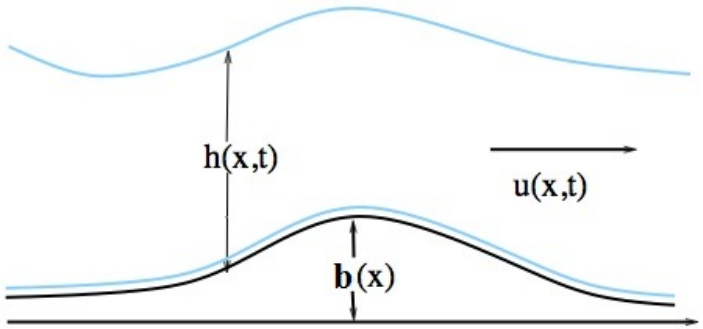

- Source terms (friction and variations of the channel width) can be added.
- Wide applications in coastal ocean, hydraulic engineering and climate.

DG methods for the SWEs

- A vast amount of literatures in Finite Volume methods for the SWEs.
- Initial work by:
  Schwaneberg and Kongeter (2000), Dawson and Proft (CMAME 2002), Giraldo, Hesthaven and Warburton (JCP 2002), Eskilsson and Sherwin (IJNMF 2004).
- Well-balanced DG methods by:
  Xing and Shu (JCP 2006, CiCP 2006), Ern, Piperno and Djadel (IJNMF 2008), Rhebergen, Bokhove and van der Vegt (JCP 2008), Kesserwani and Liang (CF 2010), Xing, Shu and Noelle (JSC 2011), Xing (JCP 2014) Duran and Marche (CF 2014). $\cdots$
- Positivity-preserving DG methods by:
  Bokhove (JSC 2005), Ern, Piperno and Djadel (IJNMF 2008), Bunya, Kubatko, Westerink and Dawson (CMAME 2009), Xing and Zhang (AWR 2010, JSC 2013), Kesserwani and Liang (JSC 2012). $\cdots$

DG methods

Denote the shallow water equations

$$h_t + (hu)_x = 0, \qquad (hu)_t + \left(hu^2 + \frac{1}{2}gh^2\right)_x = -ghb_x,$$

by

$$U_t + f(U)_x = s(h,b),$$

where $U = (h, hu)^T$, $f(U)$ is the flux and $s(h,b)$ is the source term.

DG (semi-discrete) methods

$$\int_{I_j} \partial_t U v dx - \int_{I_j} f(U)\partial_x v dx + \widehat{f}_{j+\frac{1}{2}} v(x^-_{j+\frac{1}{2}}) - \widehat{f}_{j-\frac{1}{2}} v(x^+_{j-\frac{1}{2}}) = \int_{I_j} s(h,b) v dx,$$

where $v(x)$ is a test function belonging to $V_{\Delta x}$,

$$\widehat{f}_{j+\frac{1}{2}} = F(U(x^-_{j+\frac{1}{2}}, t), U(x^+_{j+\frac{1}{2}}, t)),$$

and $F(a_1, a_2)$ is a numerical flux, for example, the simple Lax-Friedrichs flux.

Well-balanced methods

$$\int_{I_j} \partial_t U^n v dx - \int_{I_j} f(U^n) \partial_x v dx + \widehat{f}^l_{j+\frac{1}{2}} v(x^-_{j+\frac{1}{2}}) - \widehat{f}^r_{j-\frac{1}{2}} v(x^+_{j-\frac{1}{2}}) = \int_{I_j} s(h^n, b) v dx.$$

Well-balanced fluxes (Hydrostatic reconstruction)

After computing boundary values $U^{\pm}_{j+\frac{1}{2}}$, we set

$$U^{*,\pm}_{j+\frac{1}{2}} = \left(h^{*,\pm}_{j+\frac{1}{2}}, h^{*,\pm}_{j+\frac{1}{2}} u^{\pm}_{j+\frac{1}{2}}\right)^T, \quad h^{*,\pm}_{j+\frac{1}{2}} = \max\left(0, h^{\pm}_{j+\frac{1}{2}} + b^{\pm}_{j+\frac{1}{2}} - \max(b^+_{j+\frac{1}{2}}, b^-_{j+\frac{1}{2}})\right).$$

The left and right fluxes $\widehat{f}^l_{j+\frac{1}{2}}$ and $\widehat{f}^r_{j-\frac{1}{2}}$ are given by:

$$\begin{aligned}
\widehat{f}^l_{j+\frac{1}{2}} &= F(U^{*,-}_{j+\frac{1}{2}}, U^{*,+}_{j+\frac{1}{2}}) + \begin{pmatrix} 0 \\ \frac{g}{2}(h^-_{j+\frac{1}{2}})^2 - \frac{g}{2}(h^{*,-}_{j+\frac{1}{2}})^2 \end{pmatrix}, \\
\widehat{f}^r_{j-\frac{1}{2}} &= F(U^{*,-}_{j-\frac{1}{2}}, U^{*,+}_{j-\frac{1}{2}}) + \begin{pmatrix} 0 \\ \frac{g}{2}(h^+_{j-\frac{1}{2}})^2 - \frac{g}{2}(h^{*,+}_{j-\frac{1}{2}})^2 \end{pmatrix}.
\end{aligned}$$

Note: if $b^+_{i+\frac{1}{2}} = b^-_{i+\frac{1}{2}}$, this is exactly the traditional DG method.

Well-balanced methods for the moving water

- Moving water steady state:

$$m = hu = const, \qquad E = u^2/2 + g(h+b) = const.$$

  Challenge: Nonlinearity of E.

- Conservative variables $U = (h, hu)$.
  Equilibrium variables $V = (m, E)$.

- $V = V(U, b)$ is well-defined.
  $U = U(V, b)$ is double-valued.

- To uniquely define U, define the sign function

$$\sigma := \text{sign}(Fr - 1), \qquad Fr := |u|/\sqrt{gh},$$

  The flow region is called sonic, sub- or supersonic if $\sigma = 0, -1, 1$.
  $U = U(V, b, \sigma)$ is well-defined.

Well-balanced methods for moving water (Xing JCP 2014)

$$\int_{I_j} \partial_t U^n v dx - \int_{I_j} f(U^n) \partial_x v dx + \widehat{f}^l_{j+\frac{1}{2}} v(x^-_{j+\frac{1}{2}}) - \widehat{f}^r_{j-\frac{1}{2}} v(x^+_{j-\frac{1}{2}}) = \int_{I_j} s(h^n, b) v dx,$$

Propoposition: The DG schemes described above maintain smooth moving water equilibrium exactly.

Remarks

- If the bottom is flat, i.e., $b = 0$, our well-balanced DG methods become the traditional DG methods.
- Our well-balanced methods are designed to preserve the moving water equilibrium. When applied to still water steady state, they become existing well-balanced methods presented before.

Positivity-preserving methods (Step 1)

The cell averages of the water height in the well-balanced DG methods (with a simple Euler forward time discretization):

$$\overline{h}_j^{n+1} = \overline{h}_j^n - \lambda \left[\widehat{F}\left(h^{*,-}_{j+\frac{1}{2}}, u^-_{j+\frac{1}{2}}; h^{*,+}_{j+\frac{1}{2}}, u^+_{j+\frac{1}{2}} \right) - \widehat{F}\left(h^{*,-}_{j-\frac{1}{2}}, u^-_{j-\frac{1}{2}}; h^{*,+}_{j-\frac{1}{2}}, u^+_{j-\frac{1}{2}} \right) \right],$$

where

$$\widehat{F}\left(h^{*,-}_{j+\frac{1}{2}}, u^-_{j+\frac{1}{2}}; h^{*,+}_{j+\frac{1}{2}}, u^+_{j+\frac{1}{2}} \right) = \frac{1}{2}\left(h^{*,-}_{j+\frac{1}{2}} u^-_{j+\frac{1}{2}} + h^{*,+}_{j+\frac{1}{2}} u^+_{j+\frac{1}{2}} - \alpha(h^{*,+}_{j+\frac{1}{2}} - h^{*,-}_{j+\frac{1}{2}}) \right).$$

Proposition

Consider the well-balanced DG methods above. If $h_j^n(x)$ are all non-negative, then $\overline{h}_j^{n+1}$ is also non-negative under the CFL condition ($\widehat{w}_1$ is the Gauss-Lobatto quadrature weight):

$$\lambda\alpha \le \widehat{w}_1.$$

Positivity-preserving limiter (Step 2)

$\boxed{h^n(x) \geq 0}$ $\xrightarrow[step\,1]{\text{DG update}}$ $\boxed{h^{n+1}(x) \text{ with } \overline{h}^{n+1}(x) \geq 0}$ $\xrightarrow[step\,2]{\text{limiter}}$ $\boxed{h^{n+1}(x) \geq 0}$

To enforce step 2, we introduce the following limiter on the DG polynomial

$$\widetilde{h}_j^n(x) = \theta\left(h_j^n(x) - \overline{h}_j^n\right) + \overline{h}_j^n, \qquad \theta = \min\left\{1, \frac{\overline{h}_j^n}{\overline{h}_j^n - m_j}\right\},$$

with

$$m_j = \min_{x \in I_j} h_j^n(x).$$

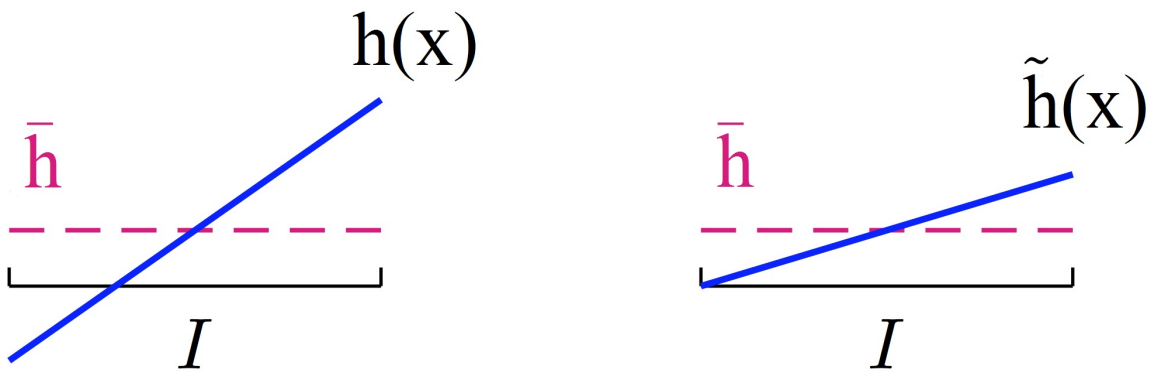

This limiter does not affect the high order accuracy and mass conservation.

Properties of this limiter

- Keeps water height non-negative;
- Preserves the local conservation of h;
- Does not destroy the high order accuracy;
- Only active in the dry or nearly dry region.

Comments

- Works for TVD high order Runge-Kutta and multi-step time discretizations.
- Positivity preserving CFL condition is $\lambda\alpha \leq 1/6$ for $k = 2, 3$. Recall that the CFL condition for linear stability for the DG methods is $\lambda\alpha \leq 1/5$ for $k = 2$.
- Any other positivity-preserving exact or approximate Rieman solver, including Godunov, Boltzmann type and Harten-Lax-Van Leer, can also be used.

Two-dimensional shallow water system

$$\begin{cases} h_t + (hu)_x + (hv)_y = 0 \\ (hu)_t + \left(hu^2 + \frac{1}{2} g h^2 \right)_x + (huv)_y = -ghb_x \\ (hv)_t + (huv)_x + \left(hv^2 + \frac{1}{2} g h^2 \right)_y = -ghb_y. \end{cases}$$

- Still water at rest steady state:

$$h + b = const, \qquad hu = 0, \qquad hv = 0.$$

- Both well-balanced and positivity-preserving techniques can be extended to 2D.

- Works for both rectangular and triangular meshes.

Summary

Constructed and tested DG methods for the Euler equations.

- Well-balanced approaches to perform efficiently near the steady state:
  1. Isothermal equilibrium state,
  2. Polytropic equilibrium state.
- A simple positivity-preserving limiter based on high order DG methods:
  1. Preserve the mass conservation,
  2. Does not affect the high order accuracy for the general solutions.

Constructed and tested DG methods for the shallow water equations.

- Well-balanced approaches to perform efficiently near the steady state:
  1. Still water at rest steady state,
  2. Moving water steady state.
- A simple positivity-preserving limiter based on high order DG methods:

High order finite difference and finite volume WENO methods have also been designed for these models.

References

- Y. Xing, X. Zhang and C.-W. Shu, **Positivity-preserving high order well-balanced discontinuous Galerkin methods for the shallow water equations**, *Advances in Water Resources*, v33 (2010), pp.1476-1493.
- Y. Xing and X. Zhang, **Positivity-preserving well-balanced discontinuous Galerkin methods for the shallow water equations on unstructured triangular meshes**, *Journal of Scientific Computing*, v57 (2013), pp. 19-41.
- Y. Xing, **Exactly well-balanced discontinuous Galerkin methods for the shallow water equations with moving water equilibrium**, *Journal of Computational Physics*, v257 (2014), pp. 536-553.
- G. Li and Y. Xing, **Well-balanced discontinuous Galerkin methods for the Euler equations under gravitational fields**, *Journal of Scientific Computing*, v67 (2016), pp. 493-513.
- S. Qian, G. Li, F. Shao and Y. Xing, **Positivity-preserving well-balanced discontinuous Galerkin methods for the shallow water flows in open channels**, *Advances in Water Resources*, v115 (2018), pp. 172-184.
- G. Li and Y. Xing, **Well-balanced discontinuous Galerkin methods with hydrostatic reconstruction for the Euler equations with gravitation**, *Journal of Computational Physics*, v352 (2018), pp. 445-462.
- X. Wen, W.S. Don, Z. Gao and Y. Xing, **Entropy stable and well-balanced discontinuous Galerkin methods for the nonlinear shallow water equations**, *Journal of Scientific Computing*, v83 (2020), 66.
- K. Wu and Y. Xing, **Uniformly high-order structure-preserving discontinuous Galerkin methods for Euler equations with gravitation: Positivity and well-balancedness**, *SIAM Journal on Scientific Computing*, in press.
- W. Zhang, Y. Xing, Y. Xia and Y. Xu, **High-order positivity-preserving well-balanced discontinuous Galerkin methods for Euler equations with gravitation on unstructured meshes**, preprint.

Acknowledgements:

Support by NSF is gratefully acknowledged.

Thank you!